

UNITED STATES DEPARTMENT OF INTERIOR
GEOLOGICAL SURVEY

Submarine Ferromanganese Deposits from the Mariana and
Volcano Volcanic Arcs, West Pacific

by

James R. Hein¹, Charlaine L. Fleishman¹, Lisa A. Morgenson¹,
Sherman H. Bloomer², and Robert J. Stern³

Open File Report 87- 281

This report is preliminary and has not been reviewed for conformity with the U.S. Geological Survey editorial standards and stratigraphic nomenclature.

¹ U.S. Geological Survey, Menlo Park

² Duke University, Durham, N.C.

³ University of Texas at Dallas, Richardson, TX

Introduction

R/V *T. Thompson* cruise TT-192 left Guam on 10 November 1985 and arrived in Sasebo, Japan, near Nagasaki, on 9 December 1985, via the Mariana and Volcano volcanic arc (Figs. 1-3). The chief scientists were R.J. Stern and S.H. Bloomer and twelve other scientists participated in the cruise (Table 1). The primary objective of the cruise was to collect samples in order to study the petrologic and geochemical evolution of the volcanic arc, especially the initial phases of arc volcanism. Samples were collected from the West Mariana Ridge and Mariana Trough for comparison (Fig. 1). These studies of petrogenesis are being conducted primarily by the two chief scientists, their students, and Drs. E. Ito and J. Morris. The participation of the senior author in the cruise was to collect and describe samples of ferromanganese deposits formed on a volcanically active island arc and to study the mechanisms of their formation. These types of ferromanganese deposits have been little studied and data are required for comparison with cobalt- and platinum-rich hydrogenetic ferromanganese deposits recovered from other areas of the Pacific basin.

The collection of ferromanganese deposits was incidental to the main objective of the cruise. Therefore, no attempt was made to sample the areas most likely to contain hydrogenetic crusts rich with cobalt and platinum within the exclusive economic zone of the west Pacific nations. Rather, this study is based on a random sampling of predominantly hydrothermal ferromanganese deposits distributed for about 1200 km along the active volcanic arc.

This report provides descriptive, mineralogical, and chemical data for the ferromanganese deposits, and a brief discussion. Chemical data include major and minor elements, rare earth elements, and platinum-group elements. A few sedimentary rocks that host much of the ferromanganese oxides were also chemically and mineralogically analyzed and those data are included (Table 4). All data were produced in the U.S. Geological Survey laboratories in Reston, Denver, and Menlo Park and the techniques are listed in the tables. More detailed discussions of the data will be presented in journal publications.

General Discussion of Pacific Ferromanganese Deposits

In the Pacific, ferromanganese deposits occur in three tectonic environments: 1) spreading axes at divergent plate margins, including back-arc basins, 2) mid-plate volcanic edifices, and 3) volcanic arcs—convergent plate margins (Hein et al., 1987). Examples of each include the East Pacific Rise, Marshall Islands, and Mariana arc system, respectively. At spreading axes, hydrothermal ferromanganese oxides form crusts on fresh basalt and are rich in manganese and poor in most trace metals. If sediment covers the spreading center, the hydrothermal fluids form iron silicates and manganese oxides within the sediment or at the sediment-seawater interface. Hydrogenetic (precipitated from ambient seawater) ferromanganese crusts enriched in cobalt, platinum, nickel, and other metals form on hard substrates of mid-plate volcanic edifices. Volcanic activity has long ceased on most of the mid-plate volcanic edifices. Where volcanism is present (hot spots) minor hydrothermal manganese may occur (for example, Loihi Seamount, south of the island of Hawaii). Volcanic arc-hosted ferromanganese deposits have been little studied and our work represents the first detailed study of these deposits from an active volcanic arc. If the Mariana-Volcano arc is typical, both hydrogenetic and hydrothermal ferromanganese deposits occur (see also Cronan et al., 1982; Moorby et al., 1984; Koski et al., 1985; Usui et al., 1986). Ferromanganese crusts on hard to soft substrates are dominantly hydrogenetic but commonly contain various amounts of admixed hydrothermal oxides, thus producing deposits with more trace metals than spreading center deposits, but less

than mid-plate deposits. Also, ferromanganese oxides form cement and stratabound layers within sedimentary rocks in volcanic arcs, and contain a different suite of enriched trace metals (including Mo, Ni, Ba, and Zn) than those of mid-plate or spreading axes deposits.

Sample Collection and Descriptions

Eighty-four dredge attempts were made (Table 2; Figs. 1-3), 76 with circular chain-bag dredges, 3 with a pipe dredge made on board ship after all the chain-bag dredges were lost, and 5 with a rectangular chain-bag dredge also made on board ship. Eighteen dredge attempts (21%) either resulted in an empty bag or lost dredge. Of the 66 dredges that recovered rocks, 18 (27%) contained significant ferromanganese deposits and 22 (33%) contained some ferromanganese oxides (Table 2). Thus, 60% of the dredge recoveries contained ferromanganese deposits.

Substrate rocks consist of intermediate to mafic volcanic rocks, volcaniclastic rocks, volcanic breccia, and minor limestone (Table 2). Volcaniclastic rocks are dominantly sandstone but range from mudstone to conglomerate. Benthic organisms, dominantly corals and silico-sponges, were recovered in several dredges (Table 2).

Ferromanganese deposits occur in five ways (Figs. 4-7): 1) Yellow-brown to black ferromanganese encrustations occur on rocks. Some of these rocks are poorly indurated mudstone (Fig. 4). The crusts are friable, layered, or laminated, and have dominantly botryoidal or granular to smooth surfaces. These deposits will be referred to as *crusts*; 2) Brown, grey, and black ferromanganese oxides cement volcaniclastic sandstone, volcanic breccia, and conglomerate (Figs. 5, 6). Sandstone is most commonly the host for these earthy, friable, black to brown cements. Rarely, the cement in breccia is grey with a metallic luster. These deposits will be referred to as *manganiferous sandstone*; 3) Manganese oxide occurs as stratiform, stratabound layers that are pale to dark grey, rarely brownish-grey, with a submetallic luster (Fig. 7); rarely the luster is metallic or glassy. These deposits occur as discrete beds or lenses, millimeters to centimeters thick, within the manganiferous sandstone. The manganese oxides are friable to dense, massive to laminated, and brittle. Pebble and cobble size chunks of these beds were recovered in several dredge hauls with only minor amounts of the associated manganiferous sandstone. This separation was due to the presence of thick manganese beds and the apparent loss of much of the friable sandstone in the process of dredging. These deposits will be referred to as *stratabound manganese*; 4) One dredge haul, D3, recovered cobbles of dark grey submetallic, irregularly shaped masses of manganese (Fig. 7A). Chemically these deposits are similar to the stratabound manganese, but differ in their texture, irregular morphology, and possibly host rock. Other than the manganese, only a small amount of red mud was recovered in D3. This manganese probably formed in much the same way as the stratabound manganese, but hydrothermal fluids debouched onto the seafloor or manganese precipitated within soft, water-saturated mud, rather than between sandstone layers within the sediment section. These deposits are considered equivalent to stratabound manganese; 5) Dredge D12, taken in the submerged caldera of Maug volcano, recovered two cobbles composed of magnetite, siderite, and goethite. In air, fresh surfaces of these black cobbles altered within days to yellow-brown goethite, reflecting the very fine grain size of the presumably hydrothermal magnetite.

Chemically, the crusts and cemented sandstones are ferromanganese oxide deposits, commonly with iron oxide more abundant than manganese oxide, whereas the stratabound manganese contains little iron and the magnetite-siderite cobbles contain little manganese.

Mineralogy

Three dominant manganese minerals occur, $\delta\text{-MnO}_2$, birnessite $[(\text{Ca},\text{Na})\text{Mn}_7\text{O}_{14} \cdot 3\text{H}_2\text{O}]$, and todorokite $[(\text{Na},\text{Ca},\text{Mn})_2\text{Mn}_5\text{O}_{12} \cdot 3\text{H}_2\text{O}]$ (Table 3). $\delta\text{-MnO}_2$ is defined by two X-ray reflections at about 2.40 Å and 1.42 Å and has also been referred to as vernadite. Birnessite has two reflections, near 7.1 Å and 3.5 Å, and todorokite also has two reflections, near 9.6 Å and 4.8 Å, but in several samples todorokite has a third reflection at 3.3 Å. These X-ray patterns occur in other marine ferromanganese deposits, except for the 3.3 Å todorokite peak. However, this third todorokite peak has been reported for samples that occur on land (ASTM file). Birnessite and todorokite that occur in abyssal manganese nodules and in on-land deposits commonly contain more X-ray reflections than those that occur in the Mariana arc samples (Burns and Burns, 1977).

Ferromanganese crust samples are predominantly $\delta\text{-MnO}_2$. Only three of the analyzed samples contain todorokite and one contains birnessite as subordinate constituents. In contrast, the manganiferous sandstones and stratabound manganese are composed of a widely varying mixture of the three manganese minerals. In four samples todorokite occurs alone, and in one breccia $\delta\text{-MnO}_2$ occurs alone. $\delta\text{-MnO}_2$, birnessite, and todorokite in the Mariana-Volcano arc samples display a wide range of crystallinities or grain size as indicated by the sharpness of the X-ray reflections. In general, the crystallinity (or grain size) of the manganese minerals is greatest in the submetallic stratabound manganese. These deposits are also the only ones that contain todorokite with three X-ray reflections. Some samples were X-rayed a second time after 9 months of exposure to the atmosphere. In some of these samples, much of the todorokite had transformed to birnessite.

Substrate rocks are dominantly composed of plagioclase and pyroxene. Some rocks also have amphibole and quartz. Secondary minerals include smectite, chlorite, illite, zeolites, goethite, calcite, and others (see Table 3). The magnetite cobbles from Maug caldera contains magnetite, siderite, goethite, aragonite, sanidine, gypsum, and lepidocrocite.

Chemical Composition

The three main types of ferromanganese deposits are chemically distinct (Tables 5-11) and can be classified according to Fe/Mn ratios. Fe/Mn ratios for crusts, manganiferous sandstones, and stratabound manganese are >1, 1.0 to 0.1, and <0.1, respectively (Tables 5, 11). Rare exceptions are noted to this classification for dredges from the Cross-Chain Seamounts and dredge D8 from Poyo Seamount. In addition, crusts are relatively rich in P, Co, Ni, Cu, Pb, V, Zn, As, Ba, and REE, and are best characterized by high Fe/Mn, P, Co, Ni, As, and REE contents (Tables 5, 6, 11).

Manganiferous sandstones are relatively enriched in Si and other terrigenous (aluminosilicate) elements, and moderately enriched in Cu, Ni, V, Zn, and Ba. REE concentrations are mostly between those of crusts and stratabound manganese, although they overlap in part with the latter. Manganiferous sandstones are best characterized by moderate Fe/Mn and high Si, Al, and Cu (Tables 5, 11).

Stratabound manganese is strongly enriched in Mn, Mo, and Ba, moderately enriched in Ni, V, and Zn, and strongly depleted in Si, Fe, and REE. It is best characterized by low Fe/Mn, Fe, and REE and by high Mn, Mo, and Ba (Tables 5, 6, 11).

Co and Ni in the crusts are correlated with both the Fe and Mn phases, in contrast to both abyssal nodules and seamount crusts (Table 10). Fe in Mariana-Volcano arc crusts is

positively correlated with Co, Ni, Pb, V, Ti, P, As, Sr, Y, Pt, and REE. Mn is positively correlated with Co, Ni, V, Sr, Cu, Mo, Zn, Cd, and Ba. This indicates that whereas Co, Ni, Sr, and V are partitioned between the Fe and Mn phases, the other elements are selectively absorbed or substituted in one of the major oxide phases. Pacific crusts typically have Co, Ni, Pb, and Zn positively correlated with the Mn phase and Cu correlated with the Fe phase (Hein et al., 1987). Pt is positively correlated with the same elements as Fe in addition to Pb and is negatively correlated with the aluminosilicate elements.

In manganiferous sandstone K, Mo, and Ba are positively correlated with Mn and Ti, P, As, Co, Cu, Pb, Zn, and Pt with Fe (Table 9). Pt is correlated with Fe, Ti, P, As, Ca, Ni, Pb, and Sr.

In stratabound manganese, Mo and some REE are positively correlated with Mn, and P and Si with Fe (Table 8). The high Mo contents are also positively correlated with As and the high Ba with Pb, Sr, and V. Pt has a perfect positive correlation with Pb and Eu and is also positively correlated with P and Pd. Pd is positively correlated with Cu, Ni, Pb, Sr, and Pt.

Three of the six platinum group elements (Pt, Pd, and Rh) vary from below their limits of detection to maximum values of 0.190, 0.015, and 0.0046 ppm, respectively (Table 5). A Pt content of 0.2 ppm is equivalent to the lowest values obtained for ferromanganese crusts from the central Pacific, which range from 0.2 to 1.2 ppm (Hein et al., 1987). Crusts contain two to three and a half times as much Pt as manganiferous sandstone and stratabound manganese, whereas, stratabound manganese has the greatest Pd content. Detectable Rh occurs only in the crusts. These relations suggest that Pt and Rh enrichments over crustal averages result from hydrogenetic (scavenging) processes and the enrichment of Pd over crustal averages results from hydrothermal (leaching) processes.

Some elements vary consistently in the ferromanganese deposits with latitude along the arc ($-15\text{--}27^\circ\text{N}$) and with depth of water (range 530-3921 m). Manganiferous sandstone and stratabound manganese show positive correlations with latitude for K and Mg respectively and negative correlations with Fe, Pb, and V and As, respectively. In contrast, crusts show a negative correlation with latitude in the aluminosilicate elements and a positive correlation with Pt, all REE, and many other metals (Table 10). Through the processes of erosion and leaching, the manganiferous sandstone and stratabound manganese reflect the arc volcanic rocks. The volcanic rocks collected during the cruise also show compositional changes with latitude, where enriched incompatible elements, especially K, Rb, and Ba, increase from 20° to 24.6° latitude, and then decrease farther to the north (P.-N. Lin et al., written communication, 1987).

In crusts, the aluminosilicate elements increase and P, Co, Mo, Ni, Pt, As, Pb, Sr, V, Zn, Y, and REE decrease with increasing depth of water (Table 10). These results are consistent for most elements with results for hydrogenetic crusts from the central Pacific (Hein et al., 1987).

Chondrite-normalized rare earth element (REE) plots also distinguish the three main types of ferromanganese deposits (Table 6; Figs. 8-11). Crusts typically have a very small negative Ce anomaly, negative Eu and Dy anomalies, in some samples a small positive Gd anomaly, and are depleted in the heavy REE relative to the light REE in the crusts. Stratabound manganese patterns are characterized by many anomalies, but an especially strong positive Tb anomaly, and depletion in light and heavy REE relative to the other ferromanganese deposits. Manganiferous sandstone patterns are depleted in both the heavy and light REE, but more so in the heavy REE. No particular pattern of anomalies is recognized.

REE patterns for all three types of ferromanganese deposits contrast with patterns for Mariana arc volcanic rocks, which lack significant anomalies, and are relatively depleted in all REE (Figs. 11, 12). The stratabound manganese patterns are most comparable to the volcanic rocks in total REE abundance.

Discussion

We provide the following general and preliminary conclusions on the origin of the Mariana-Volcano arc ferromanganese deposits. The ferromanganese crusts form from a combination of hydrogenetic and low-temperature hydrothermal precipitation of metal oxides. The relatively high cobalt, nickel, lead, phosphorus, and REE contents support this conclusion. Crust cobalt concentrations (average 0.14%, Table 11) are much higher than those found in hydrothermal deposits (<0.01%) but lower than those found in Pacific hydrogenetic deposits (average 0.6% for the Pacific; Hein et al., 1987). Using these averages, crusts contain roughly on the average a 25% hydrothermal contribution. Apparently, continuous slow hydrogenetic precipitation of metals is episodically interrupted by relatively rapid precipitation from dilute plumes of ferromanganese oxides released into the water column by submarine volcanic eruptions and hydrothermal activity. This mechanism is also supported by the distribution of crust analyses on the ternary diagram ($\text{Cu}+\text{Ni}+\text{Co}$) $10:\text{Fe}:\text{Mn}$ (Fig. 13); crusts plot in and span the boundary between the hydrogenetic and hydrothermal crust fields. The ages, growth rates, and range of relative proportion of hydrogenetic and hydrothermal layers in the crusts are not known, but analyses are in progress to determine these characteristics.

Manganiferous sandstones formed by the injection of presumably low-temperature hydrothermal fluids into a water-rich unconsolidated section of volcaniclastic sediment. The sediment ranges from mudstone to conglomerate. The manganese impregnated the interstitial spaces and formed a matrix and cement for the rocks. The rocks are friable to well cemented with Mn contents ranging from about 4% to 20%. Rarely, the manganese also replaces part of the host sediment. Manganiferous sandstones are relatively high in aluminosilicate phases, manganese, and copper and low in iron.

The stratabound manganese formed by the same mechanism as the manganiferous sandstones, but presumably closer to the hydrothermal fluid-producing vent (fissure) or at higher temperature. Although most of this submetallic manganese is stratiform, what we infer to be feeder systems are oriented perpendicular to bedding. Stratabound manganese layers have very high manganese contents, up to 48% Mn (76% MnO_2), average 40% Mn, but also contain significant amounts of other metals, especially Mo, Ni, Ba, and Zn. These high trace metal contents are unlike hydrothermal manganese deposits that occur as crusts on basalt at oceanic spreading axes. Few data are available for Mo contents of spreading-axes crusts, but those available range from 90-1100 ppm (Hein, unpublished data; Grill et al., 1981). High Zn and Ba contents probably best distinguish the island-arc hosted hydrothermal manganese from the spreading axes hydrothermal manganese. We suggest that trace element enrichment results from hydrothermal leaching of the arc volcaniclastic deposits and from the primary composition of the fluids. The molybdenum enrichment is not noted in the bulk chemical compositions of the manganiferous sandstones because of dilution by the large silicate fraction, but is evident in all the stratabound manganese layers. A similar origin for the stratabound manganese and manganiferous sandstone deposits is supported by the common distribution of analyses within the hydrothermal field on Figure 13.

Hydrothermal submetallic manganese deposits from the Lau Basin—Tonga Ridge areas are also enriched in Mo (average 0.15%), but not in Ni or Zn (Hein, unpublished data, 1986). This difference between the trace metal contents in deposits from the two volcanic arc systems probably resulted from differences in the composition of the host volcanic rocks.

Manganese mineralization of the sandstones occurred within the past million years, most likely during the past 700,000 years based on the age of the host sediment. Nannofossils and planktonic foraminifera from dredges D55 and D56 show no reworking and no species older than late Quaternary (D. Bukry and P. Quintero, U.S. Geological Survey, personal

communication, 1987). Other samples are being dated, but based on the similarity of samples along the active arc, we believe that most of the manganiferous sandstone and stratabound manganese mineralization is quite young. Therefore, ferromanganese mineralization occurred during late-stage volcanic processes on the active Mariana-Volcano volcanic arc, probably dominantly from submarine-subsediment flank fissure eruptions. The mineralization is likely an ongoing process along the present active arc. The mineralizing environment must also have been oxidizing as MnO₂ is a significant part of nearly all deposits; the few deposits containing only todorokite may have formed under less oxic conditions, although fluid composition was probably the main controlling factor.

Economic Considerations

Not enough data were collected in any one area to make a meaningful economic appraisal of the ferromanganese deposits. The lack of necessary data is attributed to the fact that this study was incidental to the primary objective of the cruise, as stated in the introduction. However, the data presented here offer some insights into the processes of island arc mineralization which can be used in the planning of future cruises dedicated to the study of the economic potential of the Guam—Northern Mariana Islands areas.

The best place to look for the cobalt- and platinum-rich ferromanganese crusts characteristic of the central equatorial Pacific is on the old seamounts of the Pacific plate, east of the Mariana Trench. These features were not sampled during this cruise. Based on the criteria developed by Hein et al. (1987), at least 15 seamounts or seamount complexes on the Pacific plate in this area warrant exploration. These seamount deposits may contain potentially economic concentrations of Co, Ni, Pt, and possibly other metals.

On the active Mariana arc, four types of deposits occur: 1) Manganiferous sandstones represent extensive deposits that would be classified as large-tonnage but low-grade (average 17% Mn) manganese deposits. The only metal of long-term economic potential is manganese, the most abundant trace metal other than iron being Cu, which averages 0.04%; 2) Stratabound manganese occurs throughout the length of the arc but in localized deposits, and would be classified as a low- to medium-tonnage, high-grade (average 40% Mn) manganese deposit; the average grade approaches the so-called battery grade manganese. In addition to manganese, molybdenum and in places other metals offer a long-term economic potential especially if the price of Molybdenum increased on the world market. In some samples, Mo contents are greater than those considered as ore grade (0.1%) for large on-land deposits; 3) Crust deposits are widespread, but are of lower grade than central equatorial Pacific crust deposits. Regardless, average values of 0.14% and 0.13% for cobalt and nickel are significant and suggest that richer crust deposits may occur along the active arc. The economic potential of these deposits would be the cobalt and nickel contents; 4) Magnetite-siderite deposits were recovered from the only caldera sampled. Other similar deposits may exist, but are likely very localized, and of little economic interest because base and precious metals are lacking.

The ferromanganese deposits of the active arc represent the distal parts of potentially extensive hydrothermal systems. The ubiquitous occurrence of the ferromanganese deposits suggests that polymetallic sulfide deposits may also crop out in places on uplifted parts of the arc. The sulfide deposits represent the deeper parts of the same hydrothermal systems that produced the ferromanganese oxides, or the laterally more proximal deposits to the vents. Appropriately chosen sampling sites may yield sulfide deposits. In addition, polymetallic sulfides may occur in the Mariana Trough associated with back-arc spreading systems.

In summary, of the metallic deposits listed, cobalt-rich crusts on the seamounts of the

Pacific plate probably have the greatest economic potential, with the crusts on the active arc and the molybdenum-rich deposits of secondary importance.

Acknowledgments

We thank the captain and crew of the R/V *T. Thompson* for a very successful cruise despite often difficult weather conditions. Sample collection occurred during a cruise funded by NSF, OCE-841579 and OCE-8415699. We appreciate Robin Smith's help in processing ferromanganese samples while at sea. We would especially like to thank chemists Floyd Brown, Fred Lichte, and Steve Wilson and all of the analysts referenced in the chemistry tables for providing the excellent chemical data reported here. We thank David Bukry, Paula Quinterno, and Ellen Moore of the U.S. Geological Survey for identifying nannofossils, foraminifera, a pelecypod, and brachiopod in the volcaniclastic sandstones. We thank David Clague, Randolph Koski, and Tracy Vallier, all at U.S. Geological Survey, for reviewing this manuscript.

References Cited

- Bloomer, S.H., 1983, Distribution and origin of igneous rocks from the landward slopes of the Marianas Trench: Implication for its structure and evolution: *Jour. Geophys. Res.*, v. 88, p. 7411-7428.
- Bonatti, E., Kraemer, T., and Rydell, H., 1972, Classification and genesis of submarine iron-manganese deposits, *in:* Horn, D.R., (ed.), *Ferromanganese deposits on the ocean floor*: Washington, D.C., National Science Foundation, p. 149-166.
- Bonatti, E., Kolla, V., Moore, W.S., and Stern, C., 1979, Metallogenesis in marginal basins: Fe-rich basal deposits from the Philippine Sea: *Marine Geology*, v. 32, p. 21-37.
- Burns, R.G., and Burns, V.M., 1979, Manganese oxides, *in:* Burns, R.G. (ed.), *Marine Minerals*: Mineral. Soc. Amer. Strat. Course Notes, v. 6, p. 1-46.
- Chase, T.E., and Menard, H.W. (compilers), 1973, Bathymetric atlas of the North Pacific Ocean: U.S. Naval Oceanographic Office, Washington, D.C., Publ. No. 1301-2-3.
- Cronan, D.S., Glasby, G.P., Moorby, S.A., Thomson, J., Knedler, K.E., and McDougall, J.C., 1982, A submarine hydrothermal manganese deposit from the south-west Pacific island arc: *Nature*, v. 298, p. 456-458.
- Dixon, T.H., and Stern, R.J., 1983, Petrology, chemistry, and isotopic composition of submarine volcanoes in the southern Mariana arc: *Geol. Soc. Amer. Bull.*, v. 94, p. 1159-1172.
- Grill, E.V., Chase, R.L., MacDonald, R.D., and Murray, J.W., 1981, A hydrothermal deposit from Explorer Ridge in the northeast Pacific Ocean: *Earth and Planetary Sci. Letts.*, v. 52, p. 142-150.

Hein, J.R., Morgenson, L.A., Clague, D.A., and Koski, R.A., 1987, Cobalt-rich ferromanganese crusts from the Exclusive Economic Zone of the United States and nodules from the oceanic Pacific, *in*: Scholl, D.W., Grantz, A., and Vedder, J. (eds.), Geology and resource potential of the continental margin of western North America and adjacent ocean basins: Circum-Pacific Council for Energy and Mineral Resources, Earth Science Series, Houston Texas.

Koski, R.A., Hein, J.R., Bouse, R.M., and Sliney, R.E., 1985, Composition and origin of ferromanganese crusts from Tonga platform, southwest Pacific, *in*: Scholl, D.W., and Vallier, T.L. (eds.), Geology and offshore resources of Pacific island arcs—Tonga region: Circum-Pacific Council for Energy and Mineral Resources, Earth Science Series, Houston, Texas, v. 2, p. 179-186.

Moorby, S.A., Cronan, D.S., and Glasby, G.P., 1984, Geochemistry of hydrothermal Mn-oxide deposits from the S.W. Pacific island arc: *Geochim. et Cosmochim. Acta*, v. 48, p. 433-441.

Stern, R.J., and Bibee, L.D., 1984, Esmeralda Bank: Geochemistry of an active submarine volcano in the Mariana Island Arc: *Contrib. Mineral. Petrol.*, v. 86, p. 159-169.

Toth, J.R., 1980, Deposition of submarine crusts rich in manganese and iron: *Geological Society of America Bulletin*, v. 91, p. 44-54.

Usui, A., Yuasa, M., Yokota, S., Nohara, M., Nishimura, A., and Murakami, F., Submarine hydrothermal manganese deposits from the Ogasawara (Bonin) arc, off the Japan Islands: *Marine Geology*, v. 73, p. 311-322.

Table 1. Scientific Personnel, R/V *T. Thompson* cruise TT-192.

Sherman H. Bloomer	Co-chief Scientist, Duke University, Durham
Robert J. Stern	Co-chief Scientist, University of Texas Dallas, Richardson
Ivan Barnes	Geologist, U.S. Geological Survey, Menlo Park
Howard C. Brooks	Geologist, Oregon Department of Geology and Mineral Industries, Baker
James R. Hein	Geologist, U.S. Geological Survey, Menlo Park
Emi Ito	Geologist, University of Minnesota, Minneapolis
Michael C. Jackson	Geologist, University of Hawaii, Honolulu
P.-N. Lin	Geologist, University of Texas Dallas, Richardson
Julie Morris	Geologist, Carnegie Institution, Washington, D.C.
Koichi Nakamura	Geological Survey Japan, Tsukuba
Yuji Nakamura	University of Tokyo, Tokyo
Christopher Proctor	Geologist, Duke University, Durham
Roberta L. Smith	Geologist, Duke University, Durham
Tracy L. Vallier	Geologist, U.S. Geological Survey, Menlo Park

Table 2. Location and description of dredge hauls from the Northern Mariana and Volcano Volcanic Arcs, Cruise TT-192.

Dredge No.	Location	Latitude °N	Longitude °E	Water Depth (m)	Sample Weight (kg)	Description of Ferromanganese Oxides	Substrate Description and Benthic Organisms
D1	Ruby Volcano Begonia Peak	15°35.2'	145°32.9'	1240-	950	None	Black, glassy, plagioclase-phric basaltic andesite; coral, sponge, red crabs, and encrusting foraminifera.
		15°36.4'	145°33.6'	750			
D2	Ruby Volcano Keeler Peak	15°38.7'	145°34.4'	1400-	<1	None	No rocks recovered; black and golden coral; annelid.
		15°39.6'	145°34.7'	1000			
D3	SW Guguan Ridge	17°08.9'	145°39.4'	2975-	6	Fragments of hydrothermal cobbles and pebbles, black granular and porous, to massive and glassy or submetallic; encrusting forams. Small piece of red mud substrate which also stains cobbles and pebbles.	Red to orange-brown mud.
		17°10.4'	145°39.1'	2860			
D4	SW Guguan Ridge	17°13.78'	145°41.54'	2470-	0	No recovery	No recovery
		17°14.18'	143°41.49'	2325			
D5	Daon Seamount	17°54.96'	145°27.64'	2550-	275	None	Weathered hornblende andesite talus.
		17°55.99'	145°28.71'	1935			
D6	Daon Seamount	17°56.18'	145°30.2'	1940-	650	15% of rocks with crusts 1 mm thick, average 0.6 mm, granular-porous texture; andesite dominant crust host; encrusting forams and worm tubes.	White pumice, stratified siltstone, andesite/dacite, pyroxene basalt, thin pumice-rich bed impregnated with ferromanganese oxide.
		17°56.32'	145°29.76'	1650			
D7	Ridge SW of Agrigan Island	18°30.39'	145°32.41'	2960-	0	No recovery	No recovery
		18°29.87'	145°31.63'	2600			
D8	Poyo Seamount	19°08.97'	145°29.9'	2880-	300	50% of dredge is ferromanganese oxide cemented volcanoclastic sandstone; granular-porous texture, glassy to submetallic in places, especially where more pure oxide layers (to 6 mm thick) are intercalated; oxide pods in siltstone; crusts with botryoidal texture (average 3 mm, max. 15 mm) on volcanic breccia and minor andesite pebbles; mudstone and sandstone with crusts to 40 mm thick.	Volcanoclastic sandstone and fine breccia, one andesite cobble and several pebbles; minor mudstone.
		19°10.50'	145°30.5'	2200			
D9	Cheref Seamount	19°21.95'	145°28.2'	900-	450	None	Red massive andesite, dacite, black vesicular basalt, dark grey andesite, siltstone, sandstone; much coral.
		19°22.5'	145°27.05'	605			
D10	Cheref Seamount	19°22.48'	145°23.35'	2100-	275	None	Scoriaceous andesite, hornblende andesite, hornblende basalt.
		19°23.73'	145°24.85'	1400			

Dredge No.	Location	Latitude °N	Longitude °E	Water Depth (m)	Sample Weight (kg)	Description of Ferromanganese Oxides	Substrate Description and Benthic Organisms
D11	Chesef Seamount	19°27.3' 19°27.73'	145°29.44' 145°30.28'	1380-894	450	30% of rocks with patina <1 mm thick, except on sandstone which is cemented with oxides; more tightly cemented and coarser-grained than D8.	Vesicular basalt, massive basalt, volcaniclastic sandstone, rounded basalt pebbles; silicosponge, horn coral, branching coral, starfish, several unidentified organisms.
D12	Meng Island Caldera	20°01.52' 20°01.20'	145°13.37' 145°12.87'	172-55	400	Thin crusts (<2 mm) on volcanic rocks and patina on coral; 2 magnetite-sidrite-goethite nodules, with volcanic rock nuclei.	Aphyric basalt talus; dead coral debris.
D13	Supply Reef	20°06.72' 20°07.33'	145°02.76' 145°04.38'	1650-1060	125	Cement for sandstone slabs <5 mm thick.	98% plagioclase-olivine basalt, 2% volcaniclastic sandstone; silicosponges, crinoids.
D14	NE Supply Reef	20°07.72' 20°07.89'	145°04.64' 145°05.43'	1060-530	30	Cement for sandstone.	>99% aphyric basalt, <1% volcaniclastic sandstone.
D15	Ahyi Seamount	20°23.76' 20°24.06'	144°58.63' 144°59.08'	1930-1120	200	Patina on volcanic breccia; one breccia cemented with oxide; another breccia with 8 mm crust on top and 1 to 4 mm massive metallic layer on bottom.	98% basalt, aphyric basalt with diabase inclusions, 2% volcanic breccia-layered pale green volcaniclastic rocks.
D16	Ahyi Seamount	20°24.5' 20°24.96'	144°59.1' 144°58.98'	1100-322	4	None	Three basalt cobbles.
D17	Ahyi Seamount	20°25.33' 20°25.51'	145°10.9' 145°10.58'	360-310	0	No recovery	No recovery
D18	Makhahnas Seamount	20°34.09' 20°28.45'	144°51.5' 144°49.68'	1190-950	8	Patina on basalt.	Augite andesite, friable andesite, basalt.
D19	NW Uracas Seamount	20°34.85' 20°35.32'	144°48.41' 144°50.03'	1135-840	30	Rare minor cement in breccia.	White pumice, altered basalt, altered volcaniclastic breccia and siltstone; large soft coral(?), golden coral, silicosponge.
D20	NW Uracas Seamount	20°36.71' 20°36.96'	144°39.17' 144°38.49'	1640-1510	100	10% of dredge is volcaniclastic rocks with crusts to 8 mm. Thick, submetallic slabs, some breccias and sandstones impregnated with oxides.	White pumice, yellow pumice and pumiceous siltstone, basalt, volcaniclastic breccia and sandstone.

Dredge No.	Location	Latitude °N	Longitude °E	Water Depth (m)	Sample Weight (kg)	Description of Ferromanganese Oxides	Substrate Description and Benthic Organisms
D21	NW Uracas Ridge	20°38.89' 20°39.5'	144°26.96' 144°26.5'	2200-2000	60	Seven pieces of pumice with brownish-black crusts to 24 mm (average 13 mm) thick, subtly botryoidal and porous; texturally different granular black patina (<2mm) on volcanic rocks; encrusting forams.	Vesicular basalt, pumice.
D22	NW Uracas Ridge	20°46.69' 20°46.47'	144°28.9' 144°28.53'	1385-1150	50	Stains on pumice.	White pumice, as olivine-phyric basalt.
D23	Chamorro Seamount	20°50.5' 20°49.9'	144°42.25' 144°43.11'	1600-1380	40	Rare stains on pumice.	Fresh white pumice, andesite.
D24	Chamorro Seamount	20°49.73' 20°49.02'	144°42.28' 144°42.23'	1050-940	0	No recovery	No recovery
D25	S. Daikoku Seamount	21°02.22' 21°01.50'	144°29.62' 144°29.89'	1450-1430	150	None	Aphyric glassy basalt, vesicular basalt, plagioclase-aphyric basalt.
D26	S. Daikoku Seamount	21°01.01' 21°01.46'	144°30.56' 144°31.25'	850-500	225	None	Grey pumice, vesicular banded volcanic rock, vesicular phric basalt, glassy basalt.
D27A	Cross-Chain Seamount South	21°02.39' 21°02.40'	143°48.84' 143°49.05'	2050-2015	0	No recovery	No recovery
D27B	Cross-Chain Seamount South	21°03.09' 21°02.83'	143°49.93' 143°51.3'	2290-1610	4	Crust 6 to 16 mm (average 12 mm) thick; subtly botryoidal, much iron oxide in microcracks and between grains. Encrusting forams.	One slab of volcanic breccia.
D28	Cross-Chain Seamount South	21°08.47' 21°07.44'	143°54.25' 143°55.33'	1715-1350	90	All rocks have patina to 2 mm thick; about 1% have thicker crusts to 19 mm, average 10 mm; about 2% of dredge is massive to porous, submetallic to metallic cobbles and nodules; some pieces with up to 7 distinct layers, which reflect different episodes of deposition; some nodules mixed with iron-rich mudstone; encrusting forams.	Pumice, basalt, volcanic breccia with mafic volcanic clasts, volcanoclastic sandstone; small crab, sponge, worm tubes.
D29	S. Daikoku Seamount	21°18.61' 21°19.23'	144°11.12' 144°11.61'	920-400	450	None	Basalt and basaltic andesite with disseminated pyrite.
D30	Eifuku Seamount	21°23.73' 21°23.98'	144°08.34' 144°08.52'	975-725	275	None	Pillow basalt, vesicular basalt.

Dredge No.	Location	Latitude °N	Longitude °E	Water Depth (m)	Sample Weight (kg)	Description of Ferromanganese Oxides	Substrate Description and Benthic Organisms
D31	Eifuku Seamount	21°23.08' 21°23.8'	144°06.79' 144°06.9'	171.5- 1500	225	<1% of rocks with cement for thin slabs of sandstone.	Fresh, olivine-pyroxene basalt, fresh plagioclase basalt with pyroxene ultramafic nodules, volcanic breccia, minor volcaniclastic sandstone, disseminated sulfides, minor hydrothermal mud.
D32A	Eifuku Seamount	21°35.9' 21°36.27'	144°07.3' 144°07.6'	1830- 1750	0	No recovery	No recovery
D32B	Eifuku Seamount	21°36.29' 21°36.67'	144°07.03' 144°07.05'	1750- 1730	0	No recovery	No recovery
D33	Kasuga Seamount	21°45.87' 21°46.57'	143°43.18' 143°42.48'	1170- 600	100	95% of rocks have patina; 10% of rocks are volcanic breccia with clasts altered to orange-brown iron oxides and cemented with and veined by submetallic oxides.	Orange altered basalt, altered hornblende andesite, hyaloclastite and volcanic breccia; 1 kg white branching coral.
D34	Fukujin Seamount	21°51.89' 21°54.64'	143°27.50' 143°27.16'	1600- 1002	500	None	Plagioclase-phyric basalt, aphyric basalt, rare disseminated pyrite; coral, echinoderms.
D35	Fukujin Seamount	21°57.6' 21°57.3'	143°25.4' 143°26.07'	1075- 580	275	None	Plagioclase-phyric basaltic andesite, vesicular dark grey basalt, altered brown andesite, coralline limestone boulders.
D36	SE Syoyo Ridge	22°04.9' 22°07.38'	143°24.00' 143°23.90'	1950- 1860	250	Crusts on volcanic breccia with clay matrix (5% of rocks), rare crusts, to 30 mm thick, on volcanic rocks; encrusting forams and worm tubes.	Altered metavolcanic rocks, volcanic breccia.
D37	Syoyo Ridge	22°17.57' 22°18.01'	143°13.54' 143°13.40'	1572- 1417	110	Crusts to 37 mm, average 22 mm thick, on volcanic breccia and andesite, botryoidal texture; encrusting forams.	Altered andesite, volcanic breccia, minor pumice, mudstone.
D38	unnamed seamount west of Syoyo	22°22.16' 22°22.11'	143°07.22' 143°07.49'	1800- 1740	<1	<2 mm thick crust.	Two pieces of porphyritic basalt.
D39	Sakuyama Seamount	22°21.73' 22°21.55'	143°04.77' 143°04.69'	2082- 2080	2	One rock with patina, one with crust to 5 mm; patina on silicosponges.	Eight pumice cobbles; silicosponges.
D40	Syoyo Seamount	22°25.06' 22°07.83'	142°54.55' 142°54.79'	1635- 1390	275	Patina <2 mm thick on breccia and volcanic rocks; cement for some breccia.	Half pumice, half volcanic breccia and chloritized volcanic rocks.

Dredge No.	Location	Latitude °N	Longitude °E	Water Depth (m)	Sample Weight (kg)	Description of Ferromanganese Oxides	Substrate Description and Benthic Organisms
D41	Syoyo Ridge	22°27.7' 22°28.48'	142°59.95' 142°58.82'	1230-600	600	Patina on most rocks, cement for some breccia and pebble conglomerates, clasts are coated with as well as cemented by oxides; cobbles and pebbles are dense and laminated.	80% green and brown tuff and volcanioclastic siltstone to conglomerate, 10% volcanic cobbles and pebbles, 10% breccia and ferromanganese cobbles and pebbles; abundant coral, echinoderms, and crab.
D42	NW Syoyo Ridge	22°49.77' 22°52.77'	142°35.11' 142°36.03'	2450-1580	50	Patina on most rocks, some crusts to 20 mm thick, intercalated with siltstone.	Altered yellow, white, and green volcanioclastic and sheared metavolcanic rock, minor pumice.
D43	NW Syoyo Ridge	22°50.63' 22°51.77'	142°39.63' 142°36.74'	1302-975	5	None	70% basalt, 5% volcanioclastic rocks; 25% silicospunge and bone (whale?) fragments.
D44	small seamount NW of Syoyo Ridge	22°55.34' 22°56.54'	142°31.57' 142°31.52'	2000-1760	125	Cement for breccia and sandstone, massive, dense, and submetallic cobbles and pebbles.	Aphyric basalt, volcanioclastic sandstone, volcanic breccia, ferromanganese pebbles and cobbles, minor pumice.
D45	Nikko Seamount	23°05.16' 23°05.82'	142°15.36' 142°17.16'	1865-1310	450	None	98% glassy basalt, 2% black vesicular glass, rare pumice.
D46	Nikko Seamount	23°08.94' 23°07.72'	142°21.21' 142°21.27'	1470-1330	200	Rare patina.	Plagioclase phryic massive and vesicular basalt.
D47	Ko-Hiyoshi Seamount	23°23.64' 23°23.05'	141°59.70' 141°59.14'	2030-1600	175	All rocks have patina; minor cement in breccia.	Mostly stratified volcanioclastic mudstone to conglomerate, minor volcanic rocks, ash, and pumice.
D48	South Hiyoshi Seamount	23°27.16' 23°28.49'	141°54.14' 141°56.04'	1230-740	250	None	70% basalt, 25% dacite, 5% volcanioclastic sandstone and pumice; rare disseminated pyrite.
D49	South Hiyoshi Seamount	23°30.6' 23°30.2'	141°57.3' 141°57.0'	750-430	475	None	80% massive basalt with pipe vesicles, 5% vesicular plagioclase and clinopyroxene-phryic basalt, 5% glassy pillow basalt, 10% scoria, other volcanic rocks; coral, starfish, crinoids, encrusting worm tubes, forams, golden coral.
D50	Central Hiyoshi Knoll	23°33.0' 23°36.0'	141°48.5' 141°47.5'	1100-835	0	No recovery	No recovery
D51	Central Hiyoshi Knoll	23°35.2' 23°34.8'	141°49.5' 141°48.9'	1400-1060	5	Cement for breccia and layers of submetallic manganese in breccia.	Scoria, altered andesite, glassy basalt, tuffaceous breccia.

Dredge No.	Location	Latitude °N	Longitude °E	Water Depth (m)	Sample Weight (kg)	Description of Ferromanganese Oxides	Substrate Description and Benthic Organisms
D52	Central Hiyoshi Knoll	23°37.06' 23°37.1'	141°49.13' 141°48.5'	1105-647	250	60 kg of cobbles and pebbles, metallic and submetallic, porous to dense alternating layers; layers are commonly deformed; rare layers with glassy luster.	50% massive basalt, 50% pillow fragments, vesicular basalt, volcanioclastic sandstone and siltstone, volcanic breccia, and manganese cobbles and pebbles.
D53	North Hiyoshi Seamount	23°46.4' 23°45.9'	141°48.7' 141°47.9'	1687-1280	125	None	75% massive slabby basalt, 25% glassy scoria, volcanioclastic sandstone, siltstone, mudstone.
D54	North Hiyoshi Seamount	23°49.0' 23°49.5'	141°43.6' 141°42.9'	1640-1250	100	Cement for and intercalated with sandstone; submetallic, dense and massive layers; rare layers of resinous-brown manganese.	98% vesicular to massive plagioclase basalt, glass fragments, rare pumice; 2% volcanioclastic sandstone; silicosponge.
D55	Fukutoku Seamount	24°01.7' 24°03.3'	141°35.3' 141°35.9'	1780-1070	25	8 kg cobbles and pebbles and as cement for sandstone and breccia; cobbles are laminated to massive and submetallic; crusts on basaltic tuff.	Vesicular aphyric basalt, basaltic tuff, pumice, volcanioclastic sandstone, manganese cobbles and pebbles; starfish, bryozoan, coral, crinoids.
D56	Fukutoku Seamount	24°04.5' 24°05.1'	141°33.2' 141°33.7'	1500-1250	225	Crusts to 30 mm thick, cobbles with porous black oxide and dense-massive brownish-grey submetallic oxide. Cement in breccia. Mudstone mixed with oxide due to bioturbation.	98% tuffaceous, layered, and burrowed sandstone-siltstone and sedimentary breccia with ferromanganese crusts and interlayers; 2% pyroxene-rich basalt, black vesicular glass.
D57	Fukutoku Seamount	24°02.6' 24°05.9'	141°40.2' 141°39.5'	1730-930	300	Crust on volcanioclastic sandstone, patina on basalt; cement for, and veins in sandstone.	35% volcanioclastic sandstone, 65% pillow fragments, massive to vesicular altered basalt.
D58	Komachi Seamount	23°11.6' 23°11.8'	141°23.7' 141°24.3'	1080-740	100	Crusts on siltstone and volcanic rock; crust on one piece of limestone; crusts to 50 mm thick, average 25 mm; crust fragments without substrate; some are laminated, botryoidal surface texture, rarely smooth surface; encrusting forams and worm tubes	Orange-brown siltstone, white limestone, cobbles of volcanic rock, Fe-Mn crust fragments without substrate.
D59	South Rohan Seamount	23°05.7' 23°05.6'	141°23.3' 141°22.8'	1470-1100	100	Crusts on siltstone, 6 to 48 mm thick, average 30 mm, botryoidal; encrusting forams.	Fresh scoriaceous andesite, pale brown volcanioclastic siltstone and breccia, pumice; silicosponge.
D60	Busho Seamount	23°01.1' 23°01.9'	141°28.8' 141°28.8'	1815-1110	0	No recovery	No recovery
D61	Eiji Seamount	23°06.9' 23°06.9'	142°03.9' 142°03.9'	2250-2170	0	No recovery	No recovery

Dredge No.	Location	Latitude °N	Longitude °E	Water Depth (m)	Sample Weight (kg)	Description of Ferromanganese Oxides	Substrate Description and Benthic Organisms
D62	Lav field between south and central back-arc seamounts	22°20.7' 22°21.9'	142°37.1' 142°37.9'	3320-3200	<1	None	Pale brown pumice.
D63	Back-Arc	22°15.9' 22°18.3'	142°46.6' 142°45.7'	3835-3460	0	No recovery	No recovery
D64	Back-Arc South Seamount	22°19.8' 22°21.0'	142°46.8' 142°44.1'	3000-2295	0	No recovery	No recovery
D65	Back-Arc	21°53.8' 21°53.4'	143°05.0' 143°05.6'	3150-2530	300	None	Fresh plagioclase microphyric basalt, one large pillow tube.
D66	Back-Arc	21°46.3' 21°48.3'	143°07.90' 143°04.7'	3921-3575	9	Encrusted basalt talus.	Massive basalt with glass rind.
D67	Back-Arc	21°50.1' 21°49.6'	143°03.9' 143°02.3'	3714-3290	30	<2 mm-thick crusts on mudstone; encrusting forams.	Altered basalt, some with glass rinds; minor mudstone.
D68	Back-Arc	21°42.5' 21°42.0'	143°10.2' 143°08.6'	3385-3100	80	None	Sparingly plagioclase-phyric vesicular basalt with glassy rinds, pillow fragments.
D69	West Mariana Ridge	21°48.4' 21°48.3'	142°16.9' 142°15.8'	3844-3120	0	No recovery	No recovery
D70	West Mariana Ridge	21°48.1' 21°48.0'	142°08.0' 142°06.9'	1950-1770	0	No recovery	No recovery
D71	West Mariana Ridge	22°26.8' 22°26.3'	141°55.7' 141°54.8'	1660-1660	60	Crusts on all rock types to 45 mm thick, average 30 mm, layered, with iron oxides laced throughout.	One dacite boulder; volcanioclastic sandstone, siltstone, mudstone, volcanic breccia.
D72	Creamed Onion Shoals	23°03.3' 23°02.8'	141°44.4' 141°42.3'	1500-975	0	No recovery	No recovery
D73	Kita Io-Jima	25°07.3' 25°08.1'	141°16.4' 141°15.8'	1620-1240	275	Layers intercalated in volcanioclastic sandstone and siltstone, coarse-grained; one rock surface is coated with dense conchoidally fractured oxides fragmented into equant blocks, or microbotryoidal metallic oxide, or smooth, massive, metallic oxides; some with glassy lustre; thin crusts to 5 mm thick, botryoidal surface, on basalt, cement in sandstone.	Grey-green volcanioclastic siltstone and sandstone, massive basalt with orange staining, volcanic breccia.
D74	Kaitoku Seamount	26°01.4' 26°01.5'	141°01.8' 141°00.7'	1815-1500	0	No recovery	No recovery
D75	Kaitoku Seamount	26°04.1' 26°04.5'	141°07.9' 141°07.5'	1380-1090	30	None	Coarse-grained volcanic sand, aphyric and plagioclase-phyric basalt and andesite cobbles.

Dredge No.	Location	Latitude °N	Longitude °E	Water Depth (m)	Sample Weight (kg)	Description of Ferromanganese Oxides	Substrate Description and Benthic Organisms
D76	Kaitoku Seamount	26°04.8'	141°07.1'	1190	0	Winch broke	Winch broke; dredge never on bottom.
D77	Kaitoku Seamount	26°04.7' 26°04.8'	141°07.3' 141°07.1'	975-800	25	None	Basaltic sand, aphyric and plagioclase-phyric basalt cobbles.
D78	Kiken-cho Seamount	26°50.5'	140°40.8'	1750-	0	No recovery	No recovery
D79	Nishino-jima	27°09.1' 27°08.8'	140°56.8' 140°56.1'	1740-1720	30	None	Plagioclase-phyric basalt cobbles and pebbles.
D80	Nishino-jima	27°08.9' 27°08.9'	140°55.6' 140°55.3'	1130-1050	275	Iron oxide rinds on andesite, hydrothermal(?) mud.	Clinopyroxene-plagioclase-phyric andesite, rounded pumice.
D81	Nishino-jima	27°13.5' 27°13.8'	140°43.5' 140°43.4'	1090-950	200	None	Bioturbated volcaniclastic sandstone with some larger volcanic rock clasts; silicosponge, white branching coral, starfish, crinoids, branching golden coral, annelid.
D82	Nishino-jima	27°22.3' 27°22.8'	140°58.1' 140°58.3'	1770-1665	<1	None	Basalt pebbles.

Table 3. Minerals identified by X-ray diffraction in ferromanganese deposits and host substrate rocks from the Mariana and Volcano Volcanic Arcs.

Sample No. ¹	Major ²	Moderate	Minor or Trace	Sample Type ³
D3-3-I	$\delta\text{-MnO}_2\text{-M}^4$	Todorokite-G Birnessite-M	Quartz Plagioclase	submetallic Mn cobble, 0-2 mm outer surface
D3-3-II	$\delta\text{-MnO}_2\text{-M}$	Todorokite-G Birnessite-M	K-spar? Quartz?	submetallic Mn cobble, middle layer
D3-3-III	$\delta\text{-MnO}_2\text{-M}$	Todorokite-P Birnessite-M		submetallic Mn cobble, crystals in lense
D3-3-IV	$\delta\text{-MnO}_2\text{-M}$	Todorokite-G		submetallic Mn cobble, crystals on bottom
D3-3-V	amorphous Fe oxides Fe-oxy-hydroxides		Todorokite $\text{MnO}_2\text{-P}$ Clays?	orange mud
D6-1-I	$\delta\text{-MnO}_2\text{-M}$	Plagioclase Carbonate-apatite	Calcite?	bulk <1 mm crust
D6-5-I	$\delta\text{-MnO}_2\text{-P}$	Plagioclase Halite Pyroxene	Calcite Amphibole Quartz	bulk <2 mm crust
D6-6-I	Plagioclase Pyroxene		Quartz	bulk mudstone
D6-6-II	Amphibole	K-spar		crystal clast in mudstone
D8-1-I	Plagioclase Pyroxene	$\delta\text{-MnO}_2?$ Todorokite-P Birnessite-P	Pyrite Quartz?	bulk manganiferous sandstone
D8-5-I	$\delta\text{-MnO}_2\text{-P}$	Todorokite-G Birnessite-M	Plagioclase Calcite Pyrite Quartz?	bulk manganiferous sandstone

Sample No.	Major	Moderate	Minor or Trace	Sample Type
D8-7-I	$\delta\text{-MnO}_2\text{-P}$	Todorokite-G Birnessite-F Plagioclase Pyroxene	Quartz	bulk manganiferous sandstone
D8-7-II	$\delta\text{-MnO}_2\text{-M}$	Birnessite-M Todorokite-G	Plagioclase Quartz?	stratabound manganese
D8-12-I	$\delta\text{-MnO}_2\text{-P}$	Todorokite-G Plagioclase	Calcite Quartz	stratabound manganese mixed with Mn- sandstone, 20-30 mm
D8-12-II	Plagioclase Todorokite-G	Pyroxene	Quartz $\delta\text{-MnO}_2\text{-P}$	manganiferous sandstone 8-20 mm
D8-12-III	Plagioclase Calcite	$\delta\text{-MnO}_2\text{-P}$		Brown 0-8 mm crust
D8-20-I	$\delta\text{-MnO}_2\text{-P}$	Plagioclase	Carbonate-apatite Illite?	bulk 20 mm crust
D8-20-II	Plagioclase Pyroxene			bulk basalt
D8-20-III	Plagioclase Pyroxene		Smectite Quartz?	bulk mudstone
D11-1-I	$\delta\text{-MnO}_2\text{-P}$	Todorokite-M Plagioclase Pyroxene Birnessite-P	Quartz Calcite	manganiferous sandstone
D11-2A-I	Plagioclase Todorokite-M	Pyroxene	Quartz Calcite	Bulk manganiferous sandstone
D11-2B-I	Plagioclase Pyroxene			bulk basalt
D12-1-I	Magnetite Aragonite	Lepidocrocite Plagioclase Goethite	Siderite Gypsum	magnetite- siderite cobble, outer layer

Sample No.	Major	Moderate	Minor or Trace	Sample Type
D12-1-II	Goethite	Magnetite Siderite Plagioclase	Lepidocrocite	magnetite-siderite cobble, inner layer
D12-1-III	Magnetite Sanidine	Siderite Aragonite Goethite	Gypsum Lepidocrocite	magnetite-siderite cobble, composite
D12-1-IV	Plagioclase	Pyroxene	Quartz	basalt clast
D13-1-I	Plagioclase Todorokite-M	Pyroxene	Quartz?	bulk manganiferous sandstone
D13-1-II	Plagioclase Pyroxene		Quartz	bulk andesite
D15-1-I	Plagioclase	Pyroxene Todorokite-P	$\delta\text{-MnO}_2\text{-P}$ Quartz Analcime?	bulk 8 mm crust
D15-1-II	Plagioclase	Pyroxene	Calcite?	bulk breccia
D15-1-III	$\delta\text{-MnO}_2\text{-M}$	Todorokite-G	Plagioclase Pyroxene Quartz	stratabound manganese
D19-1-I	Plagioclase Pyroxene		Quartz Clay	bulk basalt
D19-1-II	Plagioclase Pyroxene	Smectite	Carbonate-apatite?	green alteration
D20-1-I	$\delta\text{-MnO}_2\text{-M}$	Todorokite-M		stratabound manganese
D20-2-I	$\delta\text{-MnO}_2\text{-P}$ Todorokite-G		Plagioclase	stratabound manganese
D21-1-I	$\delta\text{-MnO}_2\text{-P}$ Plagioclase		Pyroxene Smectite	bulk 12 mm crust
D21-1-II	Plagioclase Pyroxene	Quartz	Smectite and/or mixed clays	bulk pumice

Sample No.	Major	Moderate	Minor or Trace	Sample Type
D21-1-III	Plagioclase	Quartz	Illite Smectite	thin layer of mudstone between crust and pumice
D27-1-I	$\delta\text{-MnO}_2\text{-P}$	Plagioclase	Pyroxene Quartz Calcite?	bulk 12 mm crust
D27-1-II	Plagioclase Pyroxene		Quartz Illite Smectite	bulk breccia
D28-2-I	$\delta\text{-MnO}_2\text{-M}$		Quartz Plagioclase	outer 0-2 mm crust
D28-2-II	$\delta\text{-MnO}_2\text{-M}$ Birnessite-G			outer 2-6 mm crust
D28-2-III	$\delta\text{-MnO}_2\text{-M}$ Birnessite-M Todorokite-P Plagioclase	Quartz	Pyroxene Carbonate-apatite Halite?	bulk volcanic and manganese breccia with manganiferous matrix
D28-3-I	$\delta\text{-MnO}_2\text{-P}$		Plagioclase Quartz	bulk 12 mm crust
D28-4-I	$\delta\text{-MnO}_2\text{-G}$	Todorokite-G		cement supported manganiferous sandstone
D28-5-I	$\delta\text{-MnO}_2\text{-M}$	Todorokite-P Birnessite-P	Plagioclase Quartz	cement supported manganiferous sandstone
D28-6-I	$\delta\text{-MnO}_2\text{-M}$	Todorokite-M Birnessite-M	Plagioclase Quartz Calcite	cement supported manganiferous sandstone
D28-7-I	$\delta\text{-MnO}_2\text{-M}$	Todorokite-M Plagioclase	Pyroxene Quartz Calcite	bulk 30 mm crust

Sample No.	Major	Moderate	Minor or Trace	Sample Type
D28-8-I	$\delta\text{-MnO}_2\text{-M}$		Plagioclase Quartz Calcite	Bulk 4 mm crust
D31-1-I	Todorokite-P Plagioclase Pyroxene		Quartz Pyrite?	manganiferous sandstone
D33-2-1-I	$\delta\text{-MnO}_2\text{-G}$		Todorokite-M Birnessite-M Plagioclase Goethite Smectite Quartz	submetallic manganese cement and veins
D33-2-3-I	$\delta\text{-MnO}_2\text{-P}$	Plagioclase	Pyroxene Quartz Smectite Mixed clays Chlorite? Fluorapatite?	bulk manganiferous breccia
D33-2-4-I	Goethite	Illite Plagioclase	Chlorite?	bulk ferruginous breccia
D33-2-4-II	Plagioclase	Pyroxene	Smectite	volcanic clast from breccia
D33-2-4-III	Plagioclase Goethite		Smectite Quartz Chlorite?	matrix from breccia
D35-1-I	Calcite Aragonite			bulk reefal limestone
D35-M8-I	Plagioclase	Pyroxene Magnetite Hematite	Calcite? Quartz?	bulk scoria
D36-1-I	$\delta\text{-MnO}_2\text{-P}$	Plagioclase Pyroxene Quartz		bulk 23 mm crust
D36-1-II	Quartz Plagioclase		Chlorite Illite	clast in mud-supported breccia

Sample No.	Major	Moderate	Minor or Trace	Sample Type
D36-1-III	Plagioclase	Smectite Quartz Pyroxene		matrix of breccia
D36-1-IV	Plagioclase Pyroxene	Quartz	Smectite	altered clast in breccia
D36-2-I	$\delta\text{-MnO}_2\text{-P}$		Plagioclase Quartz	outer 0-13 mm crust
D36-2-II	$\delta\text{-MnO}_2\text{-P}$	Plagioclase	Quartz	inner 13-20 mm crust
D36-2-III	Quartz Plagioclase	Calcite Chlorite		bulk basalt
D36-3-I	$\delta\text{-MnO}_2\text{-P}$		Quartz Plagioclase Carbonate-apatite	bulk 29 mm crust
D36-4-I	$\delta\text{-MnO}_2\text{-P}$	Plagioclase	Quartz	bulk 25 mm crust
D36-4-II	Quartz	Chlorite Plagioclase Illite Calcite		bulk andesite
D36-5-I	$\delta\text{-MnO}_2\text{-P}$	Plagioclase	Pyroxene Quartz	bulk 5 mm crust
D36-5-II	Plagioclase	Pyroxene	Smectite Quartz?	bulk basalt
D37-1-I	$\delta\text{-MnO}_2\text{-M}$		Plagioclase Quartz	bulk 20 mm crust
D37-2-I	$\delta\text{-MnO}_2\text{-M}$		Plagioclase Quartz	bulk 30 mm crust
D37-2-II	Phillipsite or Harmotome	Smectite		green matrix of breccia
D37-2-III	Plagioclase Pyroxene	Quartz	Illite Smectite Chlorite	brown matrix of breccia

Sample No.	Major	Moderate	Minor or Trace	Sample Type
D37-2-IV	Plagioclase	Smectite		andesite clast in breccia
D37-4-I	$\delta\text{-MnO}_2\text{-M}$		Plagioclase Quartz	bulk 25 mm crust
D37-5-I	$\delta\text{-MnO}_2\text{-P}$	Plagioclase	Quartz	bulk 20 mm crust
D37-5-II	Smectite		Plagioclase? Quartz?	bulk altered andesite
D41-2B-I	$\delta\text{-MnO}_2\text{-M}$	Birnessite-G Todorokite-M	Plagioclase Quartz amorphous clay	bulk stratabound manganese
D42-1-I	$\delta\text{-MnO}_2\text{-G}$		Plagioclase Quartz	bulk 2 mm crust
D44-1-I	Birnessite-G $\delta\text{-MnO}_2\text{-P}$		Todorokite-P Plagioclase Quartz Clay	bulk manganiferous sandstone and stratabound manganese
D51-1-I	$\delta\text{-MnO}_2\text{-M}$	Birnessite-M	Todorokite-P Plagioclase Pyroxene Quartz Calcite Zeolite?	stratabound submetallic manganese
D52-4-I	$\delta\text{-MnO}_2\text{-M}$	Todorokite-G Birnessite-P	Plagioclase Pyroxene Hydroxyl-apatite Quartz?	manganiferous sandstone and stratabound manganese, 0-20 mm
D52-4-II	$\delta\text{-MnO}_2\text{-P}$ Birnessite-G		Todorokite-P	stratabound manganese 20-35 mm
D52-4-III	$\delta\text{-MnO}_2\text{-P}$ Birnessite-G		Plagioclase	manganiferous sandstone and stratabound manganese, 35-55 mm

Sample No.	Major	Moderate	Minor or Trace	Sample Type
D52-5-I	$\delta\text{-MnO}_2\text{-M}$	Todorokite-M Birnessite-M	Plagioclase Illite Chabazite	stratabound manganese
D52-9-I	$\delta\text{-MnO}_2\text{-M}$	Birnessite-G	Todorokite-M Plagioclase	bulk 45 mm crust
D54-2-I	$\delta\text{-MnO}_2\text{-P}$	Todorokite-G Plagioclase	Pyroxene Quartz	bulk manganiferous sandstone
D55-3-I	$\delta\text{-MnO}_2\text{-M}$	Todorokite-P Birnessite-M Plagioclase	Pyroxene	bulk manganiferous sandstone
D55-4-I	$\delta\text{-MnO}_2\text{-G}$ Birnessite-G		Halite	bulk stratabound manganese
D56-1-I	$\delta\text{-MnO}_2\text{-M}$	Plagioclase	Todorokite-M Birnessite-P (or Rancieite) Pyroxene	bulk manganiferous sandstone
D56-1-II	Plagioclase Pyroxene		Clays	bulk siltstone
D56-2-I	$\delta\text{-MnO}_2\text{-G}$	Todorokite-G Calcite	Plagioclase Birnessite-P Rancieite? Quartz	stratabound manganese, upper porous layer, with brachiopod
D56-2-II	$\delta\text{-MnO}_2\text{-M}$	Birnessite-M	Todorokite-p Quartz?	stratabound manganese, middle dense layer, with brachiopod
D56-2-III	$\delta\text{-MnO}_2\text{-M}$	Todorokite-G	Calcite Plagioclase	stratabound manganese, lower porous layer with brachiopod

Sample No.	Major	Moderate	Minor or Trace	Sample Type
D57-2-I	$\delta\text{-MnO}_2\text{-M}$	Todorokite-M Birnessite-P	Plagioclase Pyroxene Smectite	bulk manganiferous sandstone
D57-4-I	$\delta\text{-MnO}_2\text{-M}$	Todorokite-G	Plagioclase Quartz?	bulk manganiferous pumiceous sandstone
D58-3-I	$\delta\text{-MnO}_2\text{-M}$		Plagioclase Quartz	bulk 18 mm crust
D58-4-I	$\delta\text{-MnO}_2\text{-P}$			bulk 8 mm crust
D58-7-I	$\delta\text{-MnO}_2\text{-M}$			bulk 15 mm crust
D58-11-I	$\delta\text{-MnO}_2\text{-M}$			bulk 30 mm crust
D59-4-I	$\delta\text{-MnO}_2\text{-M}$		Plagioclase Quartz	bulk 25 mm crust
D71-1-I	$\delta\text{-MnO}_2\text{-M}$		Plagioclase Quartz	bulk 40 mm crust
D71-2-I	$\delta\text{-MnO}_2\text{-M}$		Plagioclase Pyroxene Quartz Pyrite?	bulk 35 mm crust
D71-4-I	$\delta\text{-MnO}_2\text{-M}$		Plagioclase Quartz	bulk 32 mm crust
D73-1A-I	$\delta\text{-MnO}_2\text{-P}$	Todorokite-G	Pyroxene Plagioclase Birnessite-P	bulk manganiferous sandstone
D73-1F-I	$\delta\text{-MnO}_2\text{-M}$	Todorokite-M Birnessite-P	Halite Phillipsite Mordenite? or Natrolite?	stratabound manganese, porous upper part

Sample No.	Major	Moderate	Minor or Trace	Sample Type
D73-1F-II	$\delta\text{-MnO}_2\text{-M}$	Todorokite-G	Birnessite-P amorphous phase	stratabound manganese, dense lower part
D73-2-I	$\delta\text{-MnO}_2\text{-M}$		Plagioclase Quartz Amphibole?	bulk 5 mm crust

¹ The first number indicates the dredge haul number, the second number indicates an individual rock in the dredge haul, and the Roman numeral indicates a subsample of this rock.

² Roughly, major is >25%, moderate is 5 to 25%, and minor or trace is <5%.

³ Sample intervals listed in millimeters are from the outer surface of crust, and bulk means a representative section through an entire rock or crust.

⁴ Crystallinity of $\delta\text{-MnO}_2$, birnessite, and todorokite designated as G for good, M for moderate, and P for poor.

Table 4. Chemical composition of three substrate rocks and a magnetite nodule dredged from the Mariana Islands. Totals based on loss on ignition (LOI).

	D15-1-B	D35-1-A	D56-1-A	D12-1-A
SiO ₂ (wt. %)	50.1	3.6	43.3	6.9
Al ₂ O ₃	14.1	2.6	17.8	2.34
Fe ₂ O ₃	7.84	1.26	10.3	43.59
FeO	5.00	0.22	<0.02	9.53
MgO	4.73	2.24	4.75	2.37
CaO	7.81	48.5	9.83	6.72
Na ₂ O	2.68	0.27	2.63	0.86
K ₂ O	1.26	<0.03	1.25	0.03
TiO ₂	0.59	0.13	0.69	0.13
P ₂ O ₅	0.18	0.11	0.21	0.07
MnO	1.00	0.07	2.88	0.66
LOI (900°C)	3.63	40.6	6.44	22.10
Total	98.92	99.60	100.08	99.30
H ₂ O ⁺	1.84	1.70	1.35	5.65
H ₂ O ⁻	0.60	0.82	3.26	5.66
CO ₂	0.08	39.0	0.47	10.2
S	—	—	—	4.0
As (ppm)	10	<10	20	70
Ba	194	36	348	26
Cd	<2	<2	<2	3
Ce	7	4	31	<4
Co	31	6	37	34
Cr	86	9	22	99
Cu	118	38	191	125
Li	—	—	49	—
Mo	4	<2	8	29
Ni	30	9	48	134
Pb	4	<4	6	6
Sr	261	4240	753	625
V	200	34	204	65
Y	—	—	13	—
Zn	58	13	69	16
Lithology	Volcaniclastic Breccia	Coralline Limestone	Green burrowed Siltstone	Magnetite-siderite Cobble

Dash means no data. All minor elements analyzed by induction coupled plasma emission spectroscopy (ICP); D15-1-B major oxides by X-ray fluorescence (XRF) except K₂O by ICP; D35-1-A and D56-1-A majors by XRF; D12-1-A majors by ICP except SiO₂ and K₂O by XRF; 4% sulfur is included in the total of D12-1-A, and Fe₂O₃ expressed as magnetite, Fe₃O₄, would be 42.33%. Analysts are A.J. Bartel, L. Bradley, N. Elsheimer, L. Espos, J. Taggart, D. Vivit.

Table 5. Chemical composition of ferromanganese deposits from the Mariana and Volcano volcanic arcs.

	D3-3	D8-1	D8-5-A	D8-12-A	D8-12-B	D8-12-C	D8-20	D11-1-A	D12-2	D13-1-A
Si (wt. %)	0.57	17.6	10.4	14.0	19.6	15.2	17.7	2.0	10.1	18.4
Al	0.29	0.40	3.60	4.10	7.90	5.30	6.50	0.83	4.00	6.90
Fe	0.23	8.1	16.8	12.3	5.7	14.8	4.7	1.56	2.75	4.7
Mg	0.68	6.6	1.61	2.00	1.80	1.48	2.68	1.76	2.25	2.22
Ca	2.13	6.2	3.3	2.70	8.5	3.4	6.6	1.07	3.6	6.3
Na	3.5	1.28	1.65	1.62	2.11	1.63	2.17	1.54	2.21	2.45
K	0.40	0.41	0.63	1.14	0.56	1.01	0.85	1.55	0.78	0.36
Ti	0.018	0.41	0.81	0.29	0.44	0.88	0.32	0.097	0.19	0.35
P	0.025	0.043	0.30	0.14	0.064	0.27	0.074	0.057	0.039	0.029
Mn	48.00	9.80	12.30	13.60	4.40	7.10	11.90	44.30	28.90	12.20
H ₂ O ⁻	4.6	1.5	4.7	2.6	2.3	4.0	1.2	3.9	3.0	1.2
H ₂ O ⁺	6.9	1.8	6.3	5.4	1.9	6.1	2.2	7.4	5.3	2.4
CO ₂	0.04	0.01	0.18	0.05	3.14	0.19	0.83	0.06	0.06	0.43
Fe/Mn	0.005	0.83	1.37	0.90	1.30	2.08	0.40	0.04	0.10	0.40
As (ppm)	140	10	180	90	13	120	12	110	37	<2.0
Ba	500	250	1100	2800	260	880	290	5000	1500	230
Cd	1.40	8.4	5.8	6.2	1.70	1.90	0.65	16	18	0.35
Co	25	50	930	740	18	530	140	85	12	27
Cr	3.5	140	20	35	21	24	71	5.8	15	39
Cu	28	210	580	4000	120	400	900	400	130	220
Mo	1300	73	140	230	<5	19	56	840	240	38
Ni	82	320	1200	1400	130	730	120	840	150	38
Pb	10	<50	650	300	<50	330	<50	100	<50	<50
Sr	400	210	1000	540	410	800	400	1100	530	300
V	<5	460	580	310	260	340	220	410	620	250
Zn	110	310	560	480	140	370	83	840	160	85
Y	<5	16	130	39	38	110	15	38	12	17
Ce	<10	<10	310	53	<10	210	<10	22	<10	<10
Pt	<0.005	0.005	0.084	0.026	0.007	0.039	0.006	0.054	0.010	<0.005
Pd	<0.010	0.002	0.0022	0.0024	0.0026	0.0022	0.004	0.015	0.002	0.0056
Rh	<0.001	<0.001	<0.001	<0.001	<0.001	<0.001	<0.001	<0.001	<0.001	<0.001
Lithology	SSM	MS	MS with SSM	SSM with some MS	MS	Brown FC (8mm)	Mixed yellow-brown dark-brown FC	SSM with MS	Black submetallic FC (2mm)	MS

	D15-1-A	D20-1-A	D21-1-A	D27-1-A	D28-3-A	D28-4-A	D28-6-A	D28-7-A	D33-2-3-A	D36-2-A
Si (wt. %)	15.3	1.6	12.8	2.52	20.8	15.7	15.4	8.3	0	13.0
Al	4.9	0.57	4.60	0.84	7.60	5.80	5.70	2.70	3.10	4.70
Fe	15.9	0.51	14.7	5.3	6.6	4.8	5.6	17.4	8.8	14.6
Mg	1.79	0.82	1.44	1.59	3.4	2.49	2.41	1.08	1.29	1.36
Ca	3.2	2.36	3.3	1.45	6.2	5.0	5.2	2.59	2.00	2.90
Na	1.46	3.26	1.65	1.70	2.00	2.12	2.11	1.69	0	1.82
K	0.93	0.51	0.86	1.33	0.48	0.57	0.72	0.58	0.84	1.03
Ti	0.27	0.036	0.75	0.19	0.38	0.34	0.41	0.67	0.14	0.87
P	0.16	<0.025	0.32	0.18	0.056	0.039	0.054	0.38	0.10	0.23
Mn	9.10	46.30	9.50	36.80	5.60	15.90	15.60	13.10	14.50	4.90
H ₂ O ⁻	3.6	3.0	6.9	6.2	1.5	2.6	2.0	10.3	0	14.8
H ₂ O ⁺	5.3	7.6	4.7	7.4	1.6	3.7	3.8	7.0	0	4.4
CO ₂	0.08	0.04	0.24	0.14	0.02	0.75	0.93	0.31	0	0.14
Fe/Mn	1.75	0.01	1.55	0.14	1.18	0.30	0.36	1.33	0.61	2.98
As (ppm)	180	110	150	160	12	14	19	230	0	110
Ba	850	450	970	9800	310	620	890	1100	510	760
Cd	1.85	2.75	2.20	27	0.45	7.4	16	2.30	0.30	1.10
Co	180	9	790	1000	42	33	51	1400	<5	470
Cr	26	<2.0	330	6.0	85	8.0	8.5	12	6.5	32
Ca	130	39	510	1700	140	96	190	420	45	330
Mo	190	980	100	1000	<5	67	70	170	220	<5
Ni	260	120	1500	2400	54	57	300	1700	69	380
Pb	<50	70	890	460	<50	<50	<50	1100	<50	400
Sr	360	360	930	1100	290	360	420	1200	410	670
V	230	30	390	530	260	320	460	640	320	270
Zn	220	720	400	940	110	110	390	470	320	360
Y	20	<5	120	75	17	24	34	150	35	86
Ce	17	<10	290	160	<10	<10	<10	430	17	250
Pt	0.017	<0.005	0.075	0.064	0.007	0.011	0.008	0.069	0	0
Pd	0.0026	0.001	0.0032	0.0012	0.0046	0.0024	0.0046	0.0066	0	0
Rh	<0.001	<0.001	<0.001	<0.001	<0.001	<0.001	<0.001	0.0023	0	0
Lithology	PC (8mm)	SSM	PC (12mm)	Yellow-brown PC (12mm)	PC (12mm)	Laminated SSM with admixed brown PC and MS	Submetallic MS (cement supported)	PC (30mm)	MS clasts and metallic cement and veins from breccia	Yellow-brown PC (outer layer:0-13mm)

Table 5. continued

	D36-2-B	D36-4	D37-1	D37-4	D37-5	D41-2B-A	D42-1	D44-1	D51-1	D52-4-A
Si (wt%)	12.4	12.3	7.6	9.6	9.3	1.05	4.2	7.1	5.9	8.0
Al	4.30	4.30	2.63	3.30	3.20	0.57	1.10	0.82	2.70	2.54
Fe	14.7	15.2	18.0	18.7	19.5	1.09	18.5	5.4	1.90	6.5
Mg	1.28	1.38	0.99	1.03	1.07	2.16	0.98	1.14	2.32	2.02
Ca	2.37	2.69	2.30	2.50	2.62	1.38	2.19	1.26	2.76	1.98
Na	1.49	1.43	1.55	1.80	1.67	1.69	1.74	3.1	2.7	1.78
K	1.08	1.00	0.61	0.67	0.65	1.55	0.42	0.91	1.30	1.61
Ti	0.80	0.86	0.70	0.86	0.78	0.035	0.83	0.044	0.14	0.14
P	0.23	0.25	0.43	0.42	0.44	0.031	0.47	<0.025	0.059	0.11
Mn	5.90	6.10	12.10	10.10	11.50	44.30	15.80	34.70	33.40	29.60
H ₂ O ⁻	16.7	15.8	14.4	9.7	7.3	6.2	16.2	6.2	5.1	4.4
H ₂ O ⁺	4.0	5.2	5.5	7.3	7.5	7.3	7.0	5.7	5.5	6.5
CO ₂	0.15	0.18	0.28	0.25	0.28	0.03	0.46	0.01	1.5	0.04
Fe/Mn	2.49	2.49	1.49	1.85	1.70	0.02	1.17	0.16	0.06	0.22
As (ppm)	110	120	270	250	280	78	280	50	34	57
Ba	720	760	910	980	980	2100	920	1700	870	2200
Cd	1.40	1.25	1.55	1.65	1.60	23	2.15	<0.2	10	9.8
Co	560	580	1700	1400	1600	31	2600	170	44	87
Cr	35	35	15	21	17	2.5	4.5	1.5	2.0	2.5
Cu	440	380	340	360	310	120	200	300	60	67
Mo	<5	24	18	250	160	210	1200	180	670	250
Ni	580	530	1500	1200	1400	360	2200	130	150	210
Pb	460	440	1200	1100	1300	30	1400	15	18	28
Sr	680	730	1100	1000	1200	680	1300	280	580	700
V	280	290	520	500	530	130	540	<5	160	130
Zn	360	390	430	460	460	440	530	35	190	180
Y	97	99	170	150	170	54	190	7.5	8.6	13
Ce	250	260	500	520	540	<10	750	<10	15	18
Pt	0	0	0.090	0	0	0.008	0.130	0.013	<0.005	0
Pd	0	0	0.002	0	0	0.001	0.016	0.0028	0.0012	0
Rh	0	0	0.0046	0	0	<0.001	<0.001	<0.001	<0.001	0
Lithology	Yellow-brown FC (inner layer:13- 20mm)	Yellow-brown FC (25mm)	PC (20mm)	Brown PC (25mm)	Brown PC (20mm)	Laminated SSM	PC (2mm)	SSM with MS (cement- supported)	Gray laminat- ed SSM with some MS	SSM with MS (upper layer)

	D52-4-B	D52-4-C	D52-5	D52-9	D54-2	D55-3	D55-4	D56-1-B	D56-2	D57-2
Si (wt%)	0.18	9.9	5.3	6.4	14.8	16.46	0.19	14.7	6.9	12.0
Al	0.11	4.20	0.10	2.28	6.10	5.90	0.14	6.10	2.65	3.40
Fe	0.17	3.4	6.3	3.6	6.5	4.4	0.11	5.3	1.61	9.1
Mg	1.98	2.33	1.44	2.20	3.2	1.99	2.41	2.43	1.89	2.11
Ca	1.48	3.1	1.54	1.96	5.1	3.7	1.69	4.6	7.7	2.37
Na	2.4	2.3	2.01	1.90	1.96	2.4	2.07	2.20	2.4	1.94
K	1.04	1.89	1.40	1.63	1.49	2.03	1.65	1.65	1.09	1.60
Ti	0.0085	0.23	0.072	0.13	0.43	0.30	0.01	0.35	0.13	0.16
P	<0.025	0.090	0.16	0.076	0.10	0.089	0.026	0.12	0.048	0.13
Mn	47.20	27.10	35.00	33.70	14.50	15.50	44.20	15.70	27.40	19.90
H ₂ O ⁻	4.2	2.7	6.5	4.7	2.9	2.8	5.9	2.7	3.4	4.8
H ₂ O ⁺	8.6	5.9	6.5	6.9	3.9	3.5	6.7	6.0	5.4	5.5
CO ₂	0.02	0.03	0.03	0.02	0.03	0.02	0.04	0.59	5.90	0.02
Fe/Mn	0.004	0.13	0.18	0.11	0.45	0.28	0.003	0.34	0.06	0.46
As (ppm)	28	21	98	50	14	18	48	24	20	62
Ba	530	580	1300	1300	1000	1100	900	660	910	1000
Cd	0.50	5.9	<0.2	6.9	9.6	22	13	14	4.2	12
Co	190	35	230	100	33	20	40	61	40	220
Cr	<1	12	7.0	4.5	14	17	<1.0	11	4.0	17
Cu	18	100	62	62	200	130	120	210	44	77
Mo	610	490	530	420	83	55	520	64	100	240
Ni	30	190	280	270	170	240	340	340	73	300
Pb	<10	43	38	43	23	28	10	55	20	20
Sr	450	500	520	550	800	630	590	680	620	480
V	<5	38	<5	59	310	190	150	240	81	170
Zn	18	210	140	200	220	350	260	400	85	210
Y	<5	16	6.9	12	19	22	6.9	25	13	14
Ce	<10	18	<10	27	39	53	<10	73	14	31
Pt	0	0	<0.005	0	0	0.005	0	0	0	0
Pd	0	0	0.0012	0	0	0.0022	0	0	0	0
Rh	0	0	<0.001	0	0	<0.001	0	0	0	0
Lithology	Dense brownish-gray SSM (middle layer)	SSM with MS (lower layer)	Laminated SSM	MS and SSM	MS with SSM	Bedded MS	Brown-gray to black SSM	MS with SSM	Black porous SSM with layer of brown-gray Mn and MS	MS with SSM and veins

Table 5. continued

	D57-4	D58-3	D58-4	D58-7	D58-11	D59-4	D71-1	D71-2	D71-4	D73-1A	D73-1F	D73-2
Si (wt%)	17.4	3.8	2.6	4.5	5.6	5.7	10.7	11.3	10.3	16.9	0.55	5.4
Al	7.30	1.41	0.91	1.23	1.54	1.91	3.80	2.96	3.80	5.70	0.51	1.64
Fe	5.6	20.4	20.0	20.0	19.9	21.1	17.5	18.0	17.0	6.4	0.34	19.5
Mg	3.5	1.02	1.03	0.99	1.00	0.92	1.02	1.01	1.15	2.25	2.05	1.02
Ca	6.6	2.22	2.19	2.14	2.11	2.07	2.42	2.28	2.63	4.0	1.61	2.21
Na	1.68	1.44	1.39	1.32	1.37	1.47	1.74	1.58	1.68	2.4	2.05	1.60
K	1.02	0.42	0.34	0.38	0.42	0.46	0.85	0.69	0.83	0.95	1.05	0.49
Ti	0.30	0.56	0.53	0.56	0.57	0.69	0.76	0.66	0.72	0.42	0.024	0.80
P	0.071	0.62	0.64	0.61	0.58	0.58	0.37	0.40	0.38	0.079	<0.025	0.56
Mn	10.50	16.90	17.70	16.80	15.30	13.60	9.80	11.80	10.70	12.70	45.20	15.20
H ₂ O ⁻	1.7	11.1	13.7	14.9	15.8	10.1	8.6	13.6	8.1	2.6	6.0	11.0
H ₂ O ⁺	2.8	8.1	8.3	7.8	7.4	6.2	6.7	6.1	6.6	3.5	7.7	8.4
CO ₂	0.01	0.31	0.34	0.36	0.33	0.28	0.14	0.25	0.21	0.14	0.30	0.25
Fe/Mn	0.53	1.21	1.13	1.19	1.30	1.35	1.79	1.53	1.59	0.50	0.01	1.28
As (ppm)	22	410	430	410	380	380	220	250	220	20	52	320
Ba	790	970	930	950	900	1100	910	910	910	460	5000	940
Cd	2.10	245	2.65	242	2.35	1.88	1.40	1.70	1.80	8.0	2.85	2.35
Co	220	3000	3300	3000	2600	2100	900	1100	970	31	6.4	2700
Cr	77	13	12	13	17	15	15	16	16	5.8	2.5	15
Cu	310	290	200	220	210	220	470	430	440	160	43	180
Mo	140	530	570	510	450	350	160	250	210	85	290	260
Ni	110	2000	2100	2000	1800	1500	1100	1400	1300	170	54	1900
Pb	<10	2100	240	2100	2000	1800	860	1100	870	20	<10	1600
Sr	620	1500	1500	1500	1300	1400	1000	1100	1100	430	570	1300
V	210	730	800	730	680	700	440	490	470	310	770	640
Zn	110	490	550	510	480	520	440	430	420	290	50	500
Y	13	240	240	240	220	220	150	170	150	25	18	200
Ge	15	580	570	550	520	610	380	390	360	<10	<10	830
Pt	0	0	0	0.140	0.190	0	0	0.110	0	0	0.015	0
Pd	0	0	0	0.0014	0.0014	0	0	0.002	0	0	0.0066	0
Rh	0	0	0	0.002	0.0018	0	0	0.0018	0	0	<0.001	0
Lithology	Pumiceous MS with SM layers	Black PC (18mm)	Black bo- tryoidal PC (8mm)	Black PC (15mm)	Black PC (30mm)	Dark gray PC (25mm)	Dark gray PC (40mm)	Black PC (35mm)	Mottled black and yellow- brown PC (32mm)	MS with SSM	Laminated gray to brownish- grey SSM (5mm)	Black PC

Chemistry by Induction Coupled Plasma Emission Spectroscopy.

H. Kirschenbaum and J. Marinenko provided analytical expertise; Water and CO₂ by wet chemical techniques.

Sample numbers which are identical except for the suffixes -A, -B, and -C represent different sample intervals from the same crust.

Zero means no data available; < symbol is the limit of detection.

FC, ferromanganese crust; SM, submetallic manganese; SSM, stratabound submetallic manganese; MS, manganeseiferous sandstone; Mn, manganese.

Millimeters after crusts represent crust thicknesses.

Table 6. Concentrations of Yttrium and REE (ppm) in ferromanganese deposits, Mariana Island Arc.

	D3-3	D8-1	D8-20	D21-1-A	D27-1-A	D28-4-A	D37-1	D41-2B-A	D42-1
Y	3	17	96	104	125	45	191	60	201
La	2	5	121	119	157	32	253	13	313
Ce	2	9	220	215	303	51	550	18	790
Pr	<1	1	27	27	34	6	53	2	70
Nd	<2	7	118	118	148	29	230	11	290
Sm	<0.5	2	26	26	33	6	50	2	64
Eu	0.13	0.66	6.8	6.9	8.4	1.6	12.6	0.68	16.2
Gd	1	3	29	30	37	7	56	3	68
Tb	<1	<1	5	5	6	2	8	1	10
Dy	<1	3	0	0	27	0	40	3	51
Ho	0.12	0.64	5.2	5.5	6.5	1.6	9.9	0.96	11.3
Er	<0.5	2.2	14	15	18	5.0	28	3.1	31
Tm	<0.2	0.3	2.2	2.3	2.7	0.7	4.0	0.3	4.6
Yb	<0.5	1.9	14	15	18	4.3	26	2.2	29
Lu	<0.05	0.30	2.1	2.3	2.8	0.73	4.0	0.40	4.5

	D44-1	D51-1	D52-5	D55-3	D58-7	D58-11	D71-2	D73-1F
Y	8	9	10	22	257	247	195	22
La	5	7	12	13	354	320	246	11
Ce	14	9	21	63	600	590	440	4
Pr	1	1	2	7	73	67	50	2
Nd	5	5	9	27	310	290	220	11
Sm	1	1	2	5	67	62	47	2
Eu	0.39	0.26	0.51	1.31	16.9	15.7	12.2	0.83
Gd	1	1	2	5	75	70	55	3
Tb	<1	<1	<1	<1	11	10	9	1
Dy	1	<1	<1	<1	58	54	39	3
Ho	0.40	0.24	0.37	0.76	12.9	12.3	9.8	0.73
Er	1.4	0.8	1.2	2.2	36	34	28	2.3
Tm	<0.2	<0.2	<0.2	0.3	5.2	5.0	4.1	0.3
Yb	1.5	0.8	1.0	2.3	33	32	26	2.1
Lu	0.21	0.14	0.17	0.37	5.1	5.0	4.1	0.37

Chemistry by Induction Coupled Plasma analyses; analysts were J. G. Crock, and K. Kennedy.
Zero means no data available; < symbol is the limit of detection.

Table 7. Correlation coefficient matrix for 52 samples from the Mariana Islands.
Correlations at greater than 95% confidence level are boldface.

	Si	Al	Fe	Mg	Ca	Na	K	Ti	P	Mn	H2O-	H2O+	CO2	Fe/Mn	As	Ba
Al	0.908															
Fe	0.052	-0.014														
Mg	0.473	0.262	-0.453													
Ca	0.745	0.719	-0.227	0.556												
Na	-0.092	0.005	-0.684	-0.026	0.122											
K	-0.038	0.045	-0.504	0.206	-0.164	0.126										
Ti	0.292	0.264	0.852	-0.300	0.031	-0.577	-0.444									
P	-0.372	-0.357	0.919	-0.605	-0.434	-0.603	-0.521	0.698								
Mn	-0.758	-0.670	-0.663	-0.059	-0.452	0.514	0.354	-0.779	-0.345							
H2O-	-0.368	-0.359	0.718	-0.592	-0.507	-0.484	-0.321	0.605	0.775	-0.236						
H2O+	-0.846	-0.757	0.252	-0.622	-0.802	-0.110	0.009	-0.014	0.596	0.499	0.440					
CO2	0.077	0.150	-0.164	-0.000	0.557	0.169	-0.074	-0.079	-0.153	-0.051	-0.130	-0.179				
Fe/Mn	0.291	0.241	0.816	-0.323	-0.037	-0.584	-0.389	0.889	0.584	-0.752	0.633	-0.046	-0.102			
As	-0.400	-0.387	0.835	-0.625	-0.456	-0.509	-0.568	0.558	0.959	-0.235	0.744	0.593	-0.157	0.495		
Ba	-0.376	-0.329	-0.181	-0.072	-0.358	-0.139	0.288	-0.256	-0.055	0.410	-0.028	0.317	-0.108	-0.252	-0.000	
Cd	-0.117	-0.102	-0.470	0.282	-0.110	0.096	0.600	-0.446	-0.435	0.414	-0.340	0.012	-0.086	-0.534	-0.371	0.542
Co	-0.339	-0.332	0.818	-0.509	-0.348	-0.542	-0.536	0.577	0.955	-0.290	0.737	0.512	-0.095	0.450	0.944	-0.014
Cr	0.349	0.216	0.085	0.306	0.262	-0.190	-0.140	0.211	-0.032	-0.324	-0.106	-0.373	-0.087	0.207	-0.097	-0.150
Cu	0.121	0.072	0.148	-0.022	-0.059	-0.215	0.041	0.063	0.017	-0.144	-0.045	-0.021	-0.102	0.111	0.032	0.396
Mo	-0.762	-0.699	-0.311	-0.272	-0.555	0.313	0.046	-0.508	-0.005	0.776	0.025	0.563	-0.196	-0.432	0.134	0.392
Ni	-0.329	-0.331	0.771	-0.482	-0.398	-0.599	-0.388	0.584	0.863	-0.245	0.660	0.519	-0.145	0.433	0.865	0.286
Pb	-0.144	-0.169	0.828	-0.631	-0.203	-0.568	-0.706	0.633	0.893	-0.477	0.661	0.425	-0.075	0.527	0.878	-0.111
Sr	-0.410	-0.319	0.746	-0.539	-0.410	-0.600	-0.282	0.584	0.901	-0.192	0.701	0.598	-0.082	0.419	0.589	0.186
V	-0.312	-0.363	0.638	-0.323	-0.311	-0.563	-0.612	0.473	0.806	-0.185	0.514	0.421	-0.185	0.320	0.738	0.209
Zn	-0.313	-0.305	0.455	-0.366	-0.419	-0.433	-0.120	0.383	0.553	-0.055	0.408	0.451	-0.221	0.284	0.569	0.446
Y	-0.108	0.010	0.893	-0.408	-0.170	-0.656	-0.478	0.771	0.937	-0.518	0.863	0.360	0.033	0.787	0.909	-0.022
La	-0.118	-0.012	0.905	-0.429	-0.171	-0.598	-0.514	0.784	0.949	-0.520	0.878	0.359	0.059	0.782	0.917	-0.038
Ce	-0.122	-0.018	0.889	-0.427	-0.174	-0.558	-0.490	0.811	0.915	-0.519	0.880	0.335	0.055	0.765	0.875	-0.048
Pr	-0.188	-0.046	0.898	-0.505	-0.189	-0.587	-0.590	0.785	0.940	-0.496	0.866	0.394	0.012	0.767	0.828	-0.070
Nd	-0.184	-0.043	0.900	-0.503	-0.186	-0.595	-0.595	0.785	0.941	-0.499	0.865	0.392	0.011	0.773	0.930	-0.067
Sm	-0.184	-0.047	0.899	-0.497	-0.182	-0.596	-0.599	0.788	0.938	-0.499	0.862	0.388	0.013	0.772	0.926	-0.060
Eu	-0.092	0.014	0.904	-0.418	-0.148	-0.603	-0.503	0.804	0.941	-0.541	0.862	0.332	0.055	0.790	0.899	-0.026
Gd	-0.092	0.011	0.906	-0.418	-0.151	-0.608	-0.506	0.800	0.945	-0.540	0.864	0.335	0.050	0.795	0.906	-0.026
Tb	-0.026	-0.175	0.920	-0.836	-0.182	-0.717	-0.703	0.768	0.935	-0.608	0.838	0.248	-0.019	0.769	0.965	-0.254
Dy	-0.069	0.576	0.917	-0.545	-0.135	-0.516	-0.604	0.829	0.982	-0.628	0.921	0.381	0.808	0.789	0.977	-0.230
Pd	-0.086	0.021	0.908	-0.416	-0.148	-0.620	-0.508	0.799	0.943	-0.544	0.861	0.332	0.050	0.802	0.904	-0.024
Rh	0.018	0.031	-0.385	-0.216	0.186	0.262	0.316	0.649	-0.322	-0.445	0.015	-0.710	-0.294	0.429	-0.322	-0.128
Lat	-0.250	-0.160	0.035	-0.075	-0.235	-0.067	0.369	-0.067	0.242	0.120	0.249	0.282	0.028	-0.138	0.081	-0.019
Long	0.322	0.231	-0.121	0.154	0.280	0.083	-0.275	0.034	-0.357	-0.125	-0.326	-0.358	-0.022	0.112	-0.224	0.045
Depth	0.337	0.207	0.096	0.082	0.287	0.082	-0.238	0.303	-0.103	-0.295	-0.088	-0.351	0.084	0.318	-0.133	-0.016
	Cd	Co	Cr	Ca	Mo	Ni	Pb	Sr	V	Zn	Y	La	Ce	Pr	Nd	Sm
Co	-0.328															
Cd	-0.177	-0.072														
Cu	0.098	0.081	0.096													
Mo	0.277	0.035	-0.246	-0.022												
Ni	-0.096	0.893	0.041	0.334	0.084											
Pb	-0.486	0.859	0.098	0.008	-0.150	0.792										
Sr	-0.120	0.856	-0.097	0.069	0.061	0.899	0.833									
V	-0.183	0.754	-0.055	0.061	0.018	0.724	0.813	0.721								
Zn	0.248	0.522	-0.047	0.319	0.263	0.733	0.399	0.660	0.405							
Y	-0.335	0.933	-0.021	0.240	-0.119	0.855	0.964	0.916	0.582	0.625						
La	-0.387	0.958	-0.042	0.228	-0.150	0.864	0.968	0.912	0.602	0.596	0.988					
Ce	-0.364	0.947	-0.064	0.205	-0.179	0.864	0.914	0.890	0.548	0.597	0.950	0.978				
Pr	-0.452	0.957	-0.054	0.204	-0.049	0.864	0.969	0.908	0.586	0.582	0.982	0.998	0.985			
Nd	-0.457	0.953	-0.049	0.212	-0.047	0.863	0.962	0.907	0.590	0.583	0.986	0.999	0.981	1.000		
Sm	-0.456	0.952	-0.042	0.223	-0.046	0.868	0.958	0.905	0.589	0.588	0.983	0.998	0.983	1.000		
Eu	-0.381	0.958	-0.006	0.259	-0.172	0.875	0.961	0.909	0.593	0.609	0.985	0.998	0.983	0.999	1.000	
Gd	-0.381	0.949	-0.007	0.260	-0.163	0.874	0.964	0.911	0.597	0.611	0.988	0.998	0.978	0.998	0.999	
Tb	-0.398	0.923	-0.088	0.069	-0.167	0.802	0.908	0.875	0.483	0.488	0.977	0.993	0.956	0.992	0.994	0.994
Dy	-0.478	0.971	-0.266	0.268	0.868	0.965	0.944	0.437	0.523	0.986	0.999	0.968	0.998	0.998	0.998	0.998
Ho	-0.382	0.942	0.003	0.267	-0.162	0.870	0.966	0.908	0.597	0.610	0.992	0.997	0.971	0.995	0.997	0.997
Er	-0.467	0.939	-0.032	0.225	-0.030	0.869	0.962	0.902	0.585	0.593	0.993	0.997	0.968	0.993	0.996	0.995
Tm	-0.481	0.9														

Table 8. Correlation coefficient matrix for stratabound manganese from the Mariana and Volcano volcanic arcs.
Correlations at greater than 95% confidence level are boldface.

	Si	Al	Fe	Mg	Ca	Na	K	Ti	P	Mn	H2O-	H2O+	CO2	Fe/Mn	As	Ba
Al	0.884															
Fe	0.611	0.196														
Mg	0.243	0.380	-0.008													
Ca	0.612	0.649	0.057	0.068												
Na	-0.056	0.015	-0.286	-0.670	0.203											
K	-0.079	-0.151	0.237	0.677	-0.225	-0.834										
Ti	0.943	0.929	0.474	0.315	0.549	-0.139	0.006									
P	0.276	-0.202	0.942	-0.205	-0.144	-0.230	0.238	0.114								
Mn	-0.949	-0.829	-0.588	-0.365	-0.730	0.141	-0.095	-0.878	-0.298							
H2O-	-0.374	-0.521	0.219	0.260	-0.494	-0.385	0.577	-0.448	0.384	0.232						
H2O+	-0.851	-0.805	-0.436	-0.260	-0.657	-0.052	-0.025	-0.814	-0.044	0.836	0.169					
CO2	0.431	0.469	0.028	0.134	0.927	0.068	0.009	0.414	-0.054	-0.630	-0.295	-0.531				
Fe/Mn	0.718	0.327	0.987	0.043	0.170	-0.256	0.183	0.577	0.889	-0.692	0.127	-0.537	0.107			
As	-0.385	-0.513	0.070	-0.802	-0.466	0.280	-0.276	-0.356	0.159	0.526	0.063	0.315	-0.474	-0.030		
Ba	-0.173	-0.099	-0.031	0.229	-0.310	-0.630	0.349	0.017	0.045	0.181	0.201	0.257	-0.172	-0.063	0.108	
Cd	0.277	0.290	0.546	0.527	-0.186	-0.671	0.606	0.371	0.010	-0.238	0.220	-0.299	-0.220	0.422	-0.032	0.260
Co	-0.028	-0.377	0.566	-0.039	-0.265	-0.256	0.311	-0.145	0.965	-0.004	0.278	0.265	-0.146	0.508	0.007	-0.131
Cr	0.702	0.543	0.441	0.136	0.108	-0.158	-0.239	0.640	0.104	-0.483	-0.528	-0.435	-0.209	0.536	-0.131	-0.098
Cu	0.009	0.048	0.073	0.190	-0.262	-0.604	0.486	0.253	-0.072	0.055	-0.121	0.026	-0.193	0.044	0.248	0.626
Mo	-0.612	-0.591	-0.275	-0.664	-0.526	0.245	-0.199	-0.569	-0.231	0.725	0.090	0.527	-0.515	-0.385	0.810	-0.069
Ni	-0.121	-0.163	0.163	0.127	-0.377	-0.621	0.619	0.087	0.082	0.144	0.102	0.092	-0.250	0.094	0.365	0.541
Pb	-0.122	-0.169	0.092	-0.240	-0.310	-0.298	0.060	0.132	0.239	0.272	-0.440	0.382	-0.272	0.039	0.427	0.729
Sr	0.008	0.065	0.074	0.361	-0.112	-0.732	0.659	0.260	-0.035	-0.051	0.045	-0.019	0.066	0.045	0.045	0.712
V	0.130	0.167	0.183	0.291	-0.250	-0.407	-0.126	0.170	0.111	-0.003	0.084	0.101	-0.333	0.230	-0.120	0.712
Zn	-0.204	-0.154	-0.098	-0.242	-0.295	-0.161	0.156	-0.008	-0.112	0.305	-0.266	0.234	-0.261	-0.169	0.518	0.309
Y	-0.386	-0.156	-0.223	0.518	-0.599	-0.712	0.589	-0.291	-0.316	0.273	0.518	0.483	-0.294	-0.289	-0.219	0.333
La	0.111	-0.200	0.408	0.627	-0.691	-0.997	0.867	-0.002	0.471	-0.255	0.962	0.314	-0.214	0.366	-0.452	0.522
Ce	0.467	-0.162	0.762	0.270	-0.475	-0.698	0.818	0.243	0.653	-0.518	0.763	-0.145	-0.213	0.715	-0.062	-0.191
Pr	-0.645	-0.984	0.127	-0.568	-0.988	-0.925	0.079	-0.920	0.311	0.660	0.940	0.858	-0.983	0.064	0.744	0.519
Nd	-0.862	-0.869	-0.209	-0.263	-0.943	-0.924	0.000	-0.995	-0.018	0.872	0.782	0.971	-0.897	-0.272	0.518	0.679
Sm	-0.645	-0.984	0.127	-0.568	-0.988	-0.925	0.079	-0.920	0.311	0.660	0.940	0.858	-0.983	0.064	0.744	0.519
Eu	-0.310	-0.333	0.003	0.547	-0.744	-0.872	0.540	-0.344	0.273	0.155	0.809	0.674	-0.320	-0.031	-0.430	0.874
Gd	-0.453	-0.451	-0.070	0.448	-0.841	-0.853	0.498	-0.490	0.088	0.310	0.783	0.770	-0.475	-0.120	-0.266	0.794
Ho	-0.429	-0.255	-0.188	0.586	-0.721	-0.844	0.589	-0.372	-0.144	0.283	0.685	0.654	-0.331	-0.244	-0.354	0.667
Er	-0.922	-0.532	-0.545	0.207	0.730	-0.832	0.204	-0.847	-0.538	0.928	0.459	0.849	-0.645	-0.614	0.243	0.533
Yb	-0.991	-0.521	-0.644	0.237	0.690	-0.750	-0.060	-0.892	-0.564	0.993	0.399	0.922	-0.595	-0.697	0.105	0.734
La	-0.986	-0.501	-0.653	0.260	-0.679	-0.748	-0.030	-0.877	-0.586	0.988	0.384	0.907	-0.582	-0.708	0.099	0.709
Pt	-0.247	-0.287	0.011	-0.953	-0.505	-0.662	0.498	0.051	0.965	0.342	-0.343	0.337	-0.147	-0.087	0.811	0.668
Pd	-0.329	-0.193	-0.236	0.042	-0.511	-0.543	0.355	-0.029	-0.145	0.379	-0.159	0.395	-0.186	-0.254	0.322	0.855
Lat	-0.006	-0.060	0.105	0.613	0.140	-0.407	0.527	-0.097	0.329	-0.228	0.476	0.006	0.317	0.108	-0.705	0.069
Long	0.070	0.139	-0.089	-0.525	-0.151	0.276	-0.480	0.187	-0.328	0.187	-0.552	0.005	-0.349	-0.087	0.651	0.064
Depth	-0.527	-0.436	-0.444	-0.649	-0.023	0.650	-0.419	-0.511	-0.283	0.487	0.066	0.183	0.054	-0.479	0.553	-0.150
	Cd	Co	Cr	Ct	Mo	Ni	Pb	Sr	V	Zn	Y	La	Ce	Pr	Nd	Sm
Co	-0.212															
Cr	0.385	0.095														
Cu	0.607	-0.017	0.222													
Mo	0.086	-0.052	-0.270	0.137												
Ni	0.630	0.116	0.061	0.948	0.269											
Pb	0.181	0.150	0.565	0.719	-0.223	0.689										
Sr	0.564	0.016	-0.048	0.916	-0.028	0.882	0.561									
V	0.033	-0.218	0.433	0.194	-0.348	-0.006	0.565	0.175								
Zn	0.389	-0.196	-0.009	0.693	0.474	0.728	0.899	0.523	-0.298							
Y	0.873	-0.263	-0.324	0.897	0.338	0.658	0.408	0.828	-0.312	0.837						
La	0.667	0.339	0.204	0.689	-0.289	0.638	0.931	0.790	0.148	0.414	0.661					
Ce	0.998	0.720	0.556	0.723	0.011	0.928	0.990	0.513	-0.799	0.581	0.442	0.729				
Pr	0.165	0.220	0.426	0.223	0.482	0.299	0.918	0.075	0.464	0.060	0.453	0.951	0.339			
Nd	0.165	-0.116	0.101	0.302	0.331	0.198	0.737	0.317	0.464	0.155	0.631	0.896	0.120	0.943		
Sm	0.165	0.220	0.426	0.223	0.482	0.299	0.918	0.075	0.464	0.060	0.453	0.951	0.339	1.000	0.943	
Ea	0.313	-0.035	-0.049	0.428	-0.275	0.236	0.851	0.661	0.673	0.158	0.631	0.856	0.292	0.845	0.954	0.845
Gd	0.423	-0.086	-0.062	0.537	-0.030	0.347	0.728	0.662	0.464	0.315	0.762	0.828	0.327	0.870	0.985	0.870
Ho	0.648	-0.230	-0.265	0.730	0.068	0.469	0.563	0.821	0.163	0.564	0.917	0.801	0.359	0.677	0.865	0.677
Er	0.493	-0.478	-0.326	0.626	0.741	0.316	0.275	0.758	0.132	0.537	0.918	0.732	0.049	0.668	0.855	0.668
Yb	0.228	-0.372	-0.391	0.405	0.339	0.062	0.245	0.638	0.406	0.314	0.793	0.649	-0.180	0.664	0.875	0.664
Lu	0.268	-0.583	-0.409	0.437	0.564	0.086	0.219	0.669	0.368	0.350	0.815	0.644	-0.168	0.647	0.862	0.647
Pt	-0.055	0.913	-0.105	0.928	0.194	0.878	1.000	0.944	-0.058	0.821	-1.000	-1.000	-1.000	*	*	*
Pd	0.036	0.016	-0.071	0.853	0.064	0.763	0.811	0.864	0.405	0.474	-0.125	0.042	-0.768	0.317	0.448	0.317
Lat	-0.091	0.245	-0.326	-0.330	-0.633	-0.254	-0.344	-0.048	-0.026	-0.415	0.256	0.785	0.371	0.073	0.095	0.073
Long	0.208	-0.303	0.464	0.449	0.563	0.340	0.556	0.147	0.124	0.546	-0.141	-0.730	-0.366	0.140	0.201	0.140
Depth	-0.559	-0.275	-0.605	-0.247	0.492	-0.174	-0.316	-0.247	-0.422	-0.020	-0.497	-0.984	-0.783	-0.296	-0.103	-0.296
	Ba	Gd	Ho	Er	Yb	La	Pt	Pd	Lat	Long						
Gd	0.969															
Ho	0.885	0.948														
Er	0.806	0.914	1.000													
Yb	0.899	0.945	0.972	0.965	</td											

Table 9. Correlation coefficient matrix for manganiferous sandstones from the Mariana and Volcano volcanic arcs. Correlations at greater than 95% confidence level are boldface.

Tb, Dy, Yb, and Rh deleted due to lack of data.

Table 10. Correlation coefficient matrix for ferromanganese crusts from the Mariana and Volcano volcanic arcs.
 Correlations greater than 95% confidence level are boldface.

	Si	Al	Fe	Mg	Ca	Na	K	Ti	P	Mn	H2O-	H2O+	CO2	Fe/Mn	As	Ba
Al	0.989															
Fe	-0.553	-0.590														
Mg	0.741	0.768	-0.836													
Ca	0.806	0.833	-0.668	0.901												
Na	0.565	0.606	-0.683	0.646	0.718											
K	0.395	0.406	-0.580	0.214	0.060	0.247										
Ti	-0.039	-0.040	0.540	-0.538	-0.324	-0.120	-0.045									
P	-0.806	-0.813	0.863	-0.777	-0.656	-0.640	-0.721	0.297								
Mn	-0.714	-0.698	-0.117	-0.200	-0.424	-0.159	-0.018	-0.519	0.272							
H2O-	-0.559	-0.589	0.595	-0.688	-0.663	-0.590	-0.260	0.486	0.563	0.012						
H2O+	-0.857	-0.870	0.696	-0.805	-0.811	-0.581	-0.355	0.189	0.810	0.532	0.392					
CO2	-0.156	-0.143	-0.044	-0.000	0.271	0.248	-0.313	-0.122	0.187	0.174	0.005	0.004				
Fe/Mn	0.328	0.312	0.325	-0.239	-0.154	-0.199	0.270	0.712	-0.092	-0.752	0.362	-0.162	-0.480			
As	-0.842	-0.857	0.824	-0.741	-0.684	-0.694	-0.696	0.097	0.967	0.391	0.503	0.836	0.141	-0.185		
Ba	-0.384	-0.362	-0.420	-0.002	-0.333	0.013	0.469	-0.456	-0.167	0.834	-0.138	0.239	-0.184	-0.471	-0.049	
Cd	-0.393	-0.371	-0.431	0.017	-0.316	0.005	0.447	-0.488	-0.158	0.852	-0.141	0.242	-0.158	-0.505	-0.039	0.996
Co	-0.867	-0.843	0.692	-0.625	-0.571	-0.563	-0.755	0.099	0.938	0.452	0.535	0.788	0.289	-0.302	0.932	-0.030
Cr	0.370	0.394	-0.261	0.298	0.350	0.199	0.153	0.020	-0.267	-0.233	-0.287	-0.416	-0.009	0.012	-0.345	-0.116
Ca	-0.077	-0.042	-0.665	0.186	0.001	0.334	0.653	-0.425	-0.421	0.631	-0.298	-0.073	0.120	-0.466	-0.362	0.841
Mo	-0.770	-0.757	-0.055	-0.194	-0.507	-0.308	-0.133	-0.607	0.356	0.925	0.068	0.576	-0.081	-0.670	0.517	0.733
Ni	-0.931	-0.929	0.470	-0.655	-0.714	-0.449	-0.422	0.006	0.758	0.750	0.406	0.829	0.163	-0.476	0.774	0.415
Pb	-0.503	-0.546	0.634	-0.687	-0.359	-0.370	-0.725	-0.150	0.740	0.178	0.177	0.482	0.617	-0.371	0.728	-0.219
Sr	-0.915	-0.911	0.710	-0.783	-0.731	-0.564	-0.576	0.211	0.933	0.521	0.521	0.865	0.201	-0.260	0.912	0.128
V	-0.881	-0.875	0.648	-0.637	-0.614	-0.539	-0.690	0.018	0.915	0.554	0.411	0.819	0.199	-0.383	0.928	0.122
Zn	-0.849	-0.837	0.253	-0.616	-0.815	-0.413	0.036	0.010	0.483	0.806	0.368	0.749	-0.128	-0.285	0.530	0.738
Y	-0.590	-0.675	0.832	-0.776	-0.578	-0.800	-0.793	0.378	0.932	-0.105	0.908	0.726	-0.225	0.472	0.961	-0.300
La	-0.627	-0.700	0.812	-0.757	-0.556	-0.714	-0.820	0.421	0.911	-0.088	0.916	0.721	-0.145	0.424	0.932	-0.304
Co	-0.641	-0.692	0.745	-0.728	-0.533	-0.510	-0.774	0.542	0.792	-0.081	0.899	0.641	-0.081	0.385	0.788	-0.281
Pr	-0.640	-0.706	0.803	-0.748	-0.547	-0.675	-0.827	0.449	0.899	-0.085	0.913	0.715	-0.116	0.409	0.913	-0.306
Nd	-0.633	-0.704	0.813	-0.757	-0.555	-0.697	-0.827	0.441	0.908	-0.091	0.920	0.718	-0.134	0.423	0.924	-0.308
Sm	-0.648	-0.714	0.803	-0.755	-0.558	-0.683	-0.820	0.442	0.900	-0.076	0.918	0.722	-0.130	0.408	0.917	-0.295
Eu	-0.636	-0.706	0.812	-0.758	-0.555	-0.684	-0.827	0.455	0.904	-0.091	0.921	0.718	-0.130	0.422	0.918	-0.308
Gd	-0.631	-0.707	0.823	-0.773	-0.571	-0.724	-0.820	0.435	0.918	-0.091	0.926	0.729	-0.164	0.439	0.937	-0.302
Tb	-0.598	-0.693	0.813	-0.765	-0.565	-0.706	-0.802	0.425	0.898	-0.092	0.914	0.728	-0.164	0.437	0.919	-0.301
Ho	-0.613	-0.693	0.838	-0.783	-0.575	-0.753	-0.820	0.432	0.929	-0.111	0.930	0.724	-0.187	0.467	0.949	-0.314
Er	-0.607	-0.692	0.843	-0.795	-0.587	-0.764	-0.811	0.433	0.928	-0.113	0.935	0.724	-0.209	0.482	0.951	-0.311
Tm	-0.603	-0.689	0.839	-0.783	-0.574	-0.749	-0.818	0.433	0.926	-0.115	0.931	0.723	-0.187	0.471	0.946	-0.317
Yb	-0.626	-0.789	0.836	-0.795	-0.599	-0.768	-0.801	0.420	0.928	-0.090	0.935	0.748	-0.218	0.466	0.954	-0.290
Lu	-0.630	-0.716	0.837	-0.804	-0.613	-0.773	-0.791	0.419	0.927	-0.082	0.938	0.750	-0.235	0.469	0.955	-0.279
Pt	-0.767	-0.801	0.723	-0.764	-0.701	-0.667	-0.531	0.413	0.934	0.265	0.924	0.728	0.116	0.080	0.906	-0.020
Pd	0.505	0.529	-0.260	0.429	0.537	0.525	-0.113	-0.046	-0.412	-0.413	-0.433	-0.476	0.065	0.017	-0.488	-0.319
Rh	0.018	0.331	-0.385	-0.216	0.186	0.262	0.316	0.649	-0.322	-0.445	0.015	-0.710	-0.294	0.429	-0.322	-0.128
Lat	-0.676	-0.682	0.686	-0.606	-0.610	-0.494	-0.574	0.310	0.774	0.182	0.665	0.612	-0.086	0.057	0.738	-0.109
Long	0.695	0.782	-0.679	0.693	0.590	0.524	0.613	-0.190	-0.827	-0.251	-0.603	-0.627	0.019	0.057	-0.809	0.087
Depth	0.576	0.583	-0.628	0.393	0.438	0.614	0.701	0.140	-0.731	-0.228	-0.391	-0.555	0.128	0.123	-0.812	0.111
	Cd	Co	Cr	Ca	Mo	Ni	Pb	Sr	V	Zn	Y	La	Ce	Pr	Nd	Sm
Co	-0.005															
Cr	-0.108	-0.305														
Cu	0.838	-0.314	0.065													
Mo	0.752	0.513	-0.266	0.427												
Ni	0.428	0.822	-0.166	0.136	0.728											
Pb	-0.207	0.670	-0.128	-0.393	0.205	0.498										
Sr	0.134	0.910	-0.279	-0.122	0.564	0.912	0.702									
V	0.136	0.929	-0.307	-0.162	0.629	0.876	0.649	0.954								
Zn	0.752	0.526	-0.266	0.438	0.794	0.841	0.052	0.712	0.639							
Y	-0.298	0.913	-0.564	-0.666	0.156	0.462	0.915	0.838	0.884	0.158						
La	-0.302	0.949	-0.596	-0.674	0.116	0.493	0.884	0.840	0.853	0.162						
Co	-0.282	0.892	-0.585	-0.645	0.005	0.523	0.672	0.755	0.697	0.178	0.835	0.918				
Pr	-0.302	0.968	-0.582	-0.679	0.093	0.511	0.867	0.834	0.833	0.165	0.957	0.995	0.947			
Nd	-0.305	0.954	-0.589	-0.681	0.101	0.502	0.877	0.836	0.843	0.162	0.970	0.998	0.936	0.999		
Sm	-0.292	0.959	-0.592	-0.672	0.106	0.516	0.864	0.839	0.839	0.176	0.961	0.996	0.946	1.000		
Eu	-0.306	0.955	-0.583	-0.683	0.092	0.510	0.868	0.837	0.835	0.166	0.962	0.997	0.944	1.000	0.999	1.000
Gd	-0.300	0.949	-0.587	-0.679	0.116	0.504	0.885	0.846	0.857	0.171	0.981	0.999	0.921	0.995	0.999	0.996
Tb	-0.299	0.915	-0.599	-0.665	0.112	0.489	0.854	0.837	0.837	0.166	0.974	0.996	0.898	0.982	0.986	0.983
Ho	-0.313	0.938	-0.577	-0.689	0.116	0.486	0.906	0.844	0.865	0.158	0.991	0.996	0.898	0.986	0.993	0.988
Er	-0.311	0.925	-0.584	-0.685	0.120	0.483	0.890	0.845	0.865	0.162	0.993	0.993	0.889	0.979	0.988	0.982
Tm	-0.316	0.929	-0.582	-0.689	0.112	0.480	0.894	0.840	0.859	0.154	0.992	0.995	0.895	0.983	0.991	0.986
Yb	-0.289	0.932	-0.586	-0.672	0.142	0.501	0.892	0.852								

Table 11. Statistics for Mariana and Volcano volcanic arc ferromanganese deposits.

All samples

Elements	N	Mean	Median	St. Dev.	Minimum	Maximum
Si	51	9.61	9.90	5.81	0.18	20.80
Al	52	3.26	3.15	2.22	0.10	7.90
Fe	52	9.84	6.55	7.07	0.11	21.10
Mg	52	1.81	1.69	0.96	0.68	6.60
Ca	52	3.19	2.54	1.76	1.07	8.50
Na	51	1.93	1.78	0.48	1.28	3.50
K	52	0.94	0.86	0.45	0.34	2.03
Ti	52	0.41	0.37	0.29	0.0085	0.88
P	52	0.21	0.12	0.20	<0.025	0.64
Mn	52	20.1	15.3	13.1	4.40	48.00
H ₂ O ⁻	51	6.66	4.80	4.71	1.20	16.7
H ₂ O ⁺	51	5.71	6.10	1.86	1.60	8.60
CO ₂	51	0.40	0.18	0.93	0.01	5.90
Fe/Mn	52	0.86	0.57	0.78	0.003	2.98
As	51	132	98	126	<2.0	430
Ba	52	1260	910	1520	230	9800
Cd	52	5.66	2.35	6.53	<0.2	27
Co	52	696	185	947	<5	3300
Cr	52	25.6	14.5	49.7	<1.0	330
Cu	52	334	205	583	18	4000
Mo	52	305	215	310	<5	1300
Ni	52	726	330	727	30	2400
Pb	52	453	43	634	<10	2100
Sr	52	754	650	368	210	1500
V	52	350	310	225	<5	800
Zn	52	337	360	202	18	940
Y	17	94.8	60	90.8	3	257
La	17	117	32	131	2	354
Ce	17	229	63	266	2	790
Pr	17	24.9	7	28	<1	73
Nd	17	108	29	117	<2	310
Sm	17	23.3	6	25.5	<0.5	67
Eu	17	6.0	1.6	6.4	0.13	16.9
Gd	17	26	7	28	1	75
Tb	17	4.2	2.0	4.1	<1	11
Dy	14	20.1	3.0	23.4	<1	58
Ho	17	4.7	1.6	4.8	0.12	12.9
Er	17	13.1	5.0	13.4	<0.5	36
Tm	17	1.91	0.70	1.98	<0.2	5.2
Yb	17	12.3	4.30	12.5	<0.5	33
Lu	17	1.92	0.73	1.94	<0.05	5.1
Pt	29	0.041	0.013	0.050	<0.005	0.190
Pd	29	0.0033	0.0022	0.0029	0.001	0.015
Lat	52	22.13	22.44	1.87	17.16	25.13
Long	52	143.05	142.79	1.54	141.27	145.65
Depth	52	1528	1470	567	114	2918



Submetallic Stratabound Manganese

Elements	N	Mean	Median	St. Dev.	Minimum	Maximum
Si	11	3.12	1.60	3.37	0.18	10.10
Al	11	1.13	0.57	1.34	0.10	4.00
Fe	11	1.51	1.09	1.81	0.11	6.30
Mg	11	1.80	1.98	0.59	0.68	2.41
Ca	11	2.48	1.69	1.88	1.07	7.70
Na	11	2.35	2.21	0.61	1.54	3.50
K	11	1.12	1.09	0.42	0.40	1.65
Ti	11	0.069	0.036	0.062	0.0085	0.19
P	11	0.044	0.031	0.042	<0.025	0.16
Mn	11	40.38	44.30	7.66	27.40	48.00
H ₂ O ⁻	11	4.71	4.60	1.31	3.00	6.50
H ₂ O ⁺	11	6.81	6.90	1.06	5.30	8.60
CO ₂	11	0.73	0.04	1.77	0.02	5.90
Fe/Mn	11	0.045	0.020	0.055	0.003	0.180
As	11	68.6	52.0	40.5	20	140
Ba	11	1733	910	1687	450	5000
Cd	11	8.35	4.20	8.05	<0.2	23
Co	11	64.8	40.0	75.5	6.4	230
Cr	11	4.03	2.50	4.19	<1.0	15
Cu	11	96.7	60.0	108	18	400
Mo	11	624	530	407	100	1300
Ni	11	225	150	233.6	30	840
Pb	11	30.1	20	29.8	<10	100
Sr	11	582	570	197	360	1100
V	11	214	130	267	<5	770
Zn	11	274	160	276	18	840
Y	5	20.8	10	23.0	3	60
La	5	9.0	11	4.53	2	13
Ce	5	10.8	9	8.4	2	21
Pr	5	1.5	2	0.71	<1	2
Nd	5	7.4	9	4.3	<2	11
Sm	5	1.45	2	0.80	<0.5	2.0
Eu	5	0.48	0.51	0.29	0.13	0.83
Gd	5	2.0	2	1.0	1	3
Tb	5	0.7	0.5	0.27	<1	1
Dy	5	1.5	0.5	1.4	<1	3
Ho	5	0.48	0.37	0.35	0.12	0.96
Er	5	1.53	1.2	1.16	<0.5	3.1
Tm	5	0.18	0.10	0.11	<0.2	0.3
Yb	5	1.27	1.0	0.85	<0.5	2.2
Lu	5	0.22	0.17	0.16	<0.5	0.4
Pt	8	0.013	0.0059	0.017	<0.005	0.054
Pd	8	0.0044	0.0016	0.0050	0.001	0.015
Lat	11	22.16	23.58	2.48	17.16	25.13
Long	11	143.08	141.82	1.79	141.27	145.65
Depth	11	1261	1230	683	114	2918

Manganiferous Sandstone

Elements	N	Mean	Median	St. Dev.	Minimum	Maximum
Si	17	13.81	14.80	4.11	6.40	19.60
Al	18	4.55	4.95	2.17	0.40	7.90
Fe	18	6.83	5.65	3.31	3.40	16.80
Mg	18	2.42	2.21	1.19	1.14	6.60
Ca	18	4.10	3.85	1.98	1.26	8.50
Na	17	2.06	2.11	0.42	1.28	3.10
K	18	1.11	0.99	0.53	0.36	2.03
Ti	18	0.316	0.32	0.173	0.044	0.81
P	18	0.092	0.084	0.063	<0.025	0.30
Mn	18	17.3	15.0	8.43	4.40	34.70
H ₂ O ⁻	17	3.08	2.70	1.38	1.20	6.20
H ₂ O ⁺	17	4.44	3.90	1.68	1.80	6.90
CO ₂	17	0.38	0.04	0.77	0.01	3.14
Fe/Mn	18	0.514	0.425	0.368	0.110	1.37
As	17	39.1	21	43.2	<2.0	180
Ba	18	969	840	686	230	2800
Cd	18	7.59	7.15	5.86	<0.2	22
Co	18	157	50.5	257	<5	930
Cr	18	24.5	13	34.0	1.5	140
Cu	18	393	175	909	45	4000
Mo	18	184	113	179	<5	670
Ni	18	314	200	372	38	1400
Pb	18	76.7	25	157	<10	650
Sr	18	518	490	197	210	1000
V	18	258	255	149	<5	580
Zn	18	256	215	143	35	560
Y	4	23.0	19.5	15.8	8	45
La	4	13.8	9	12.7	5	32
Ce	4	34	33	27	9	63
Pr	4	3.8	3.5	3.2	1	7
Nd	4	17.0	17	12.8	5	29
Sm	4	3.5	3.5	2.4	1	6
Eu	4	0.99	0.99	0.56	0.39	1.6
Gd	4	4.0	4.0	2.6	1	7
Tb	4	0.88	0.5	0.75	<1	2
Dy	3	1.5	1.0	1.3	<1	3
Ho	4	0.85	0.7	0.52	0.4	1.6
Er	4	2.7	2.2	1.58	1.4	5.0
Tm	4	0.35	0.3	0.25	<0.2	0.7
Yb	4	2.5	2.1	1.2	1.5	4.3
Lu	4	0.40	0.33	0.23	0.21	0.73
Pt	9	0.018	0.0080	0.026	<0.005	0.084
Pd	9	0.0030	0.0024	0.0013	0.002	0.0056
Lat	18	22.21	23.28	2.11	19.16	25.13
Long	18	143.11	142.17	1.68	141.27	145.50
Depth	18	1573	1428	596	876	2540

Ferromanganese Crusts

Elements	N	Mean	Median	St. Dev.	Minimum	Maximum
Si	23	9.61	9.60	4.95	2.52	20.80
Al	23	3.27	3.20	1.84	0.84	7.60
Fe	23	16.17	17.50	4.68	4.70	21.10
Mg	23	1.34	1.07	0.595	0.92	3.4
Ca	23	2.81	2.42	1.22	1.45	6.60
Na	23	1.63	1.63	0.20	1.32	2.17
K	23	0.712	0.670	0.271	0.34	1.33
Ti	23	0.653	0.700	0.201	0.19	0.88
P	23	0.376	0.380	0.175	0.056	0.64
Mn	23	12.49	11.80	6.54	4.90	36.80
H ₂ O ⁻	23	10.2	10.3	4.8	1.20	16.7
H ₂ O ⁺	23	6.12	6.60	1.82	1.60	8.40
CO ₂	23	0.262	0.250	0.158	0.02	0.83
Fe/Mn	23	1.53	1.53	0.62	0.14	2.98
As	23	231	230	122	12	430
Ba	23	1250	910	1874	290	9800
Cd	23	2.87	1.85	5.29	0.45	27
Co	23	1420	1100	1020	42	3300
Cr	23	36.8	16.0	66.7	4.5	330
Cu	23	401	340	328	130	1700
Mo	23	247	190	237	<5	1000
Ni	23	1289	1400	704	54	2400
Pb	23	949	890	670	<50	2100
Sr	23	1020	1100	363	290	1500
V	23	488	500	179	220	800
Zn	23	431	440	165	83	940
Y	8	177	193	62	96	257
La	8	235	249	92.9	119	354
Ce	8	464	495	206	215	790
Pr	8	50.1	51.5	19.1	27	73
Nd	8	216	225	79.1	118	310
Sm	8	46.9	48.5	16.9	26	67
Eu	8	12.0	12.4	4.17	6.8	16.9
Gd	8	52.5	55.5	18.4	29	75
Tb	8	8.00	8.50	2.39	5	11
Dy	6	44.8	45.5	11.6	27	58
Ho	8	9.18	9.85	3.06	5.2	12.9
Er	8	25.5	28.0	8.65	14	36
Tm	8	3.76	4.05	1.21	2.2	5.2
Yb	8	24.1	26.0	7.5	14	33
Lu	8	3.74	4.05	1.19	2.1	5.1
Pt	12	0.078	0.072	0.057	0.006	0.190
Pd	12	0.0027	0.0021	0.0016	0.0012	0.0066
Rh	12	0.0015	0.0008	0.0012	<0.001	0.0046
Lat	23	22.05	22.30	1.37	19.16	25.13
Long	23	142.98	143.23	1.37	141.27	145.50
Depth	23	1621	1533	461	910	2540

N is number of samples.

Figure 1. Location map of the Northern Mariana and Volcano volcanic arcs. Ship trackline indicated by solid line. Bathymetry is in fathoms.

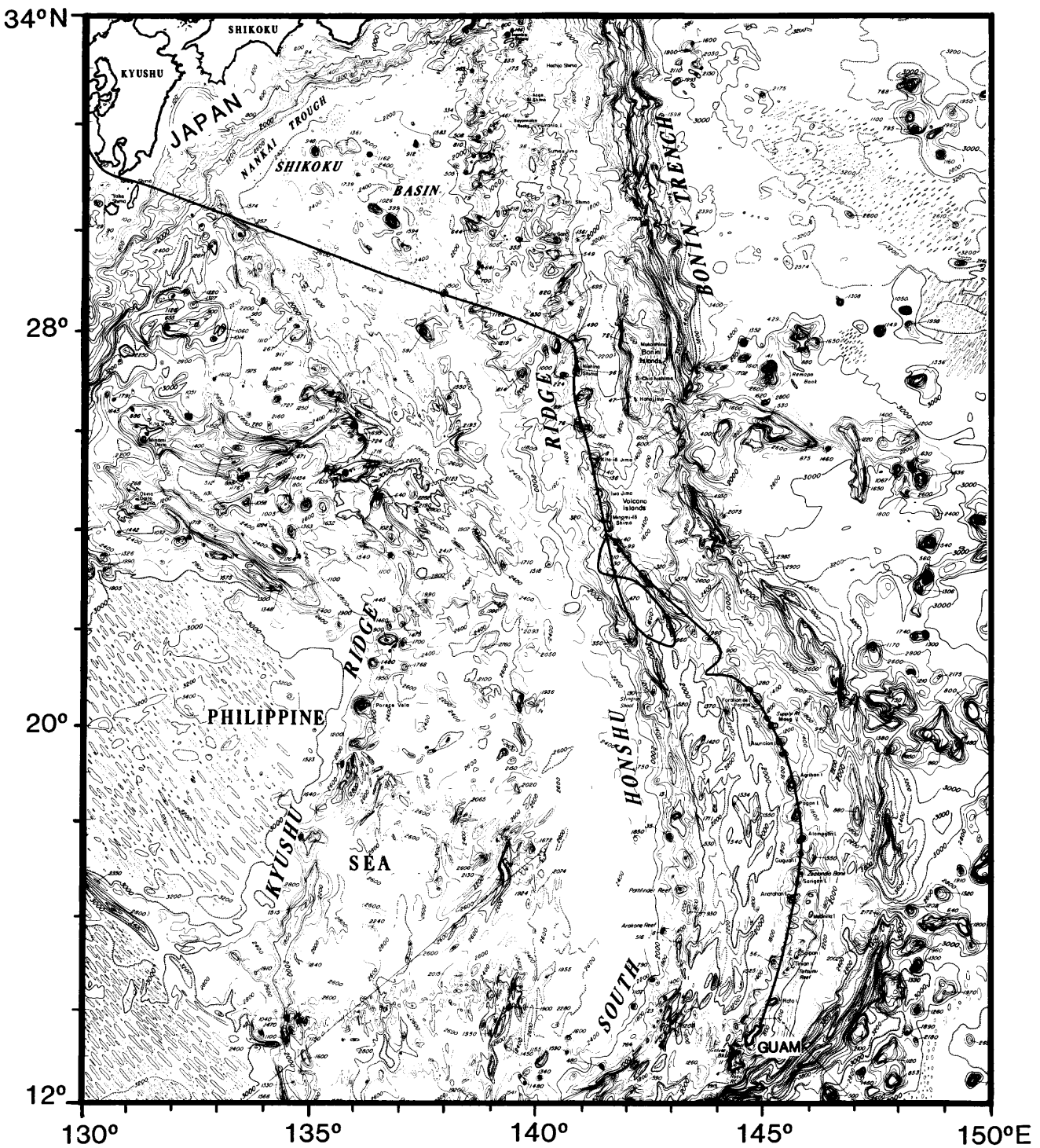


Figure 2. Sample location map of southern section (12° to 20° N Lat.) of area studied showing dredge stations. All dredge stations are numbered and correspond to dredge numbers in Table 2. Open square indicates sample recovery, but no ferromanganese rocks present. Open circle means no sample recovery. Open triangle means sample recovery included ferromanganese rocks. Base map is from Chase and Menard (1973); bathymetry is in fathoms.

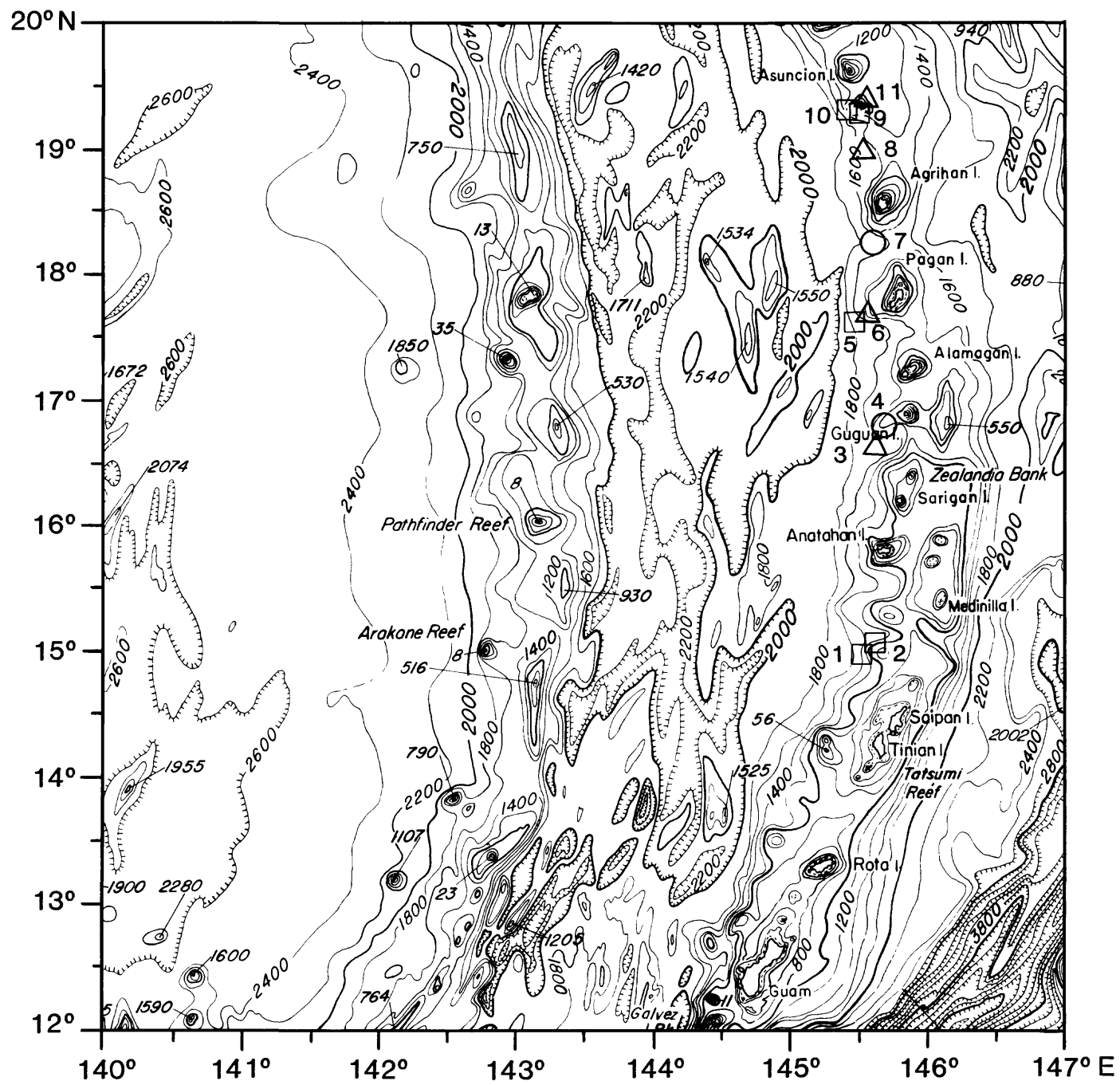


Figure 3. Sample location map of northern section (20° to 28° N Lat.) of area studied showing dredge stations. Explanation same as in Figure 2.

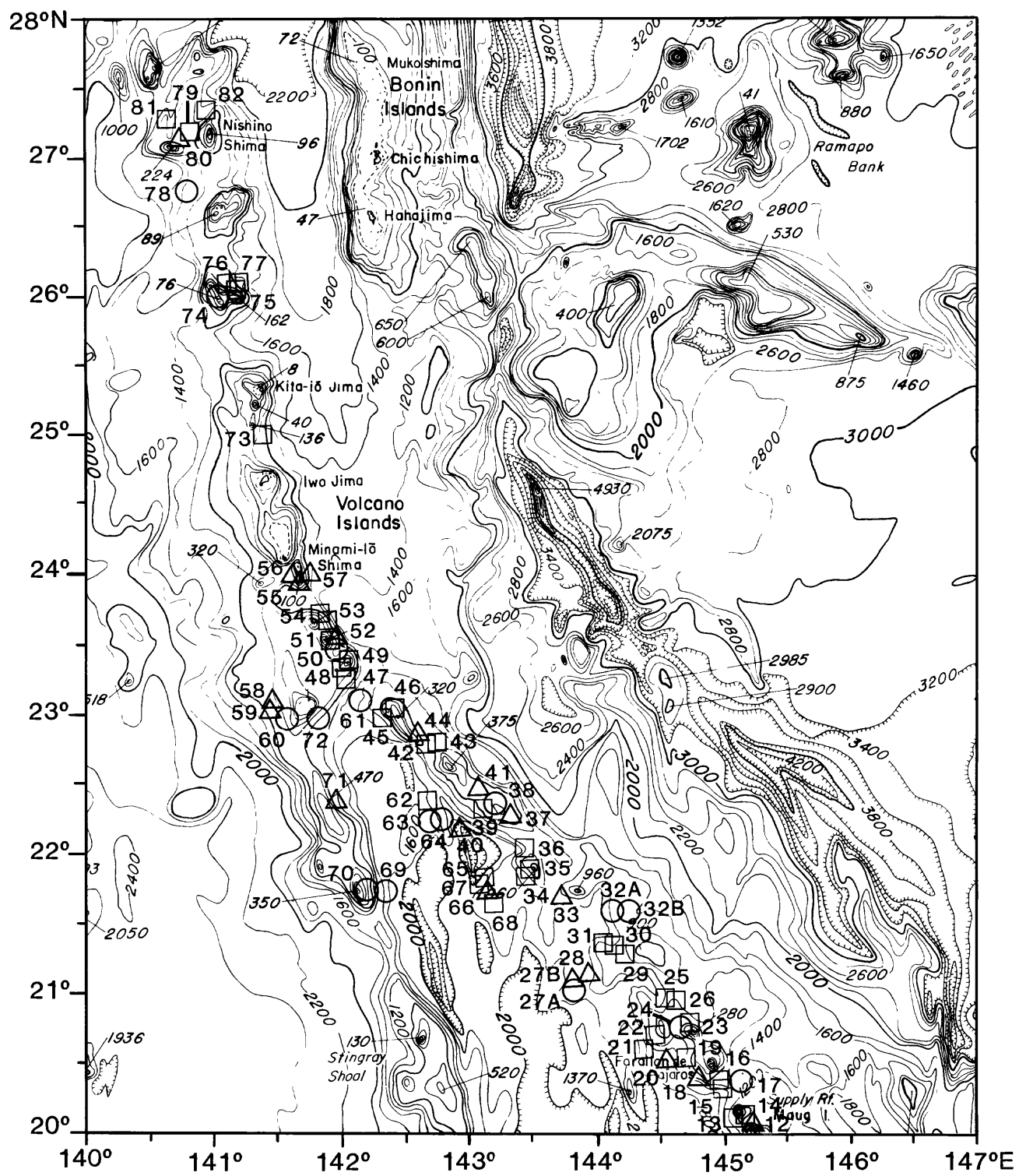


Figure 4. Ferromanganese crusts: A. D36-1, mottled yellow-brown and black, 28 mm thick crust, central upper surface. Clasts in this matrix-supported breccia are coated with oxides which partly replace the matrix. B. D37-2, black crust, average 26 mm thick, white phosphorite veins in the volcanic breccia substrate. C. D58-5, gray crust, average 12 mm thick, note botryoidal upper surface. D. D59-4, grey crust, average 25 mm thick.

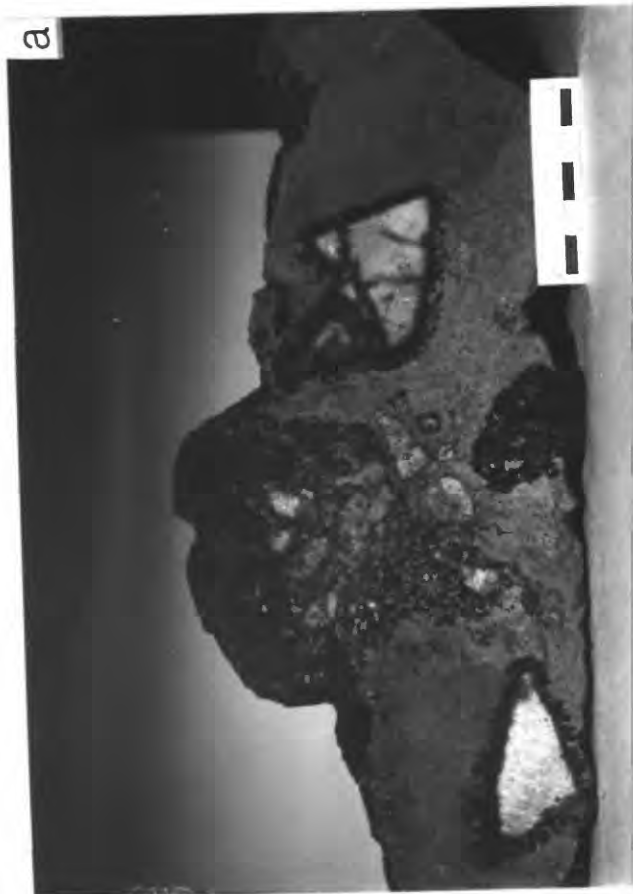
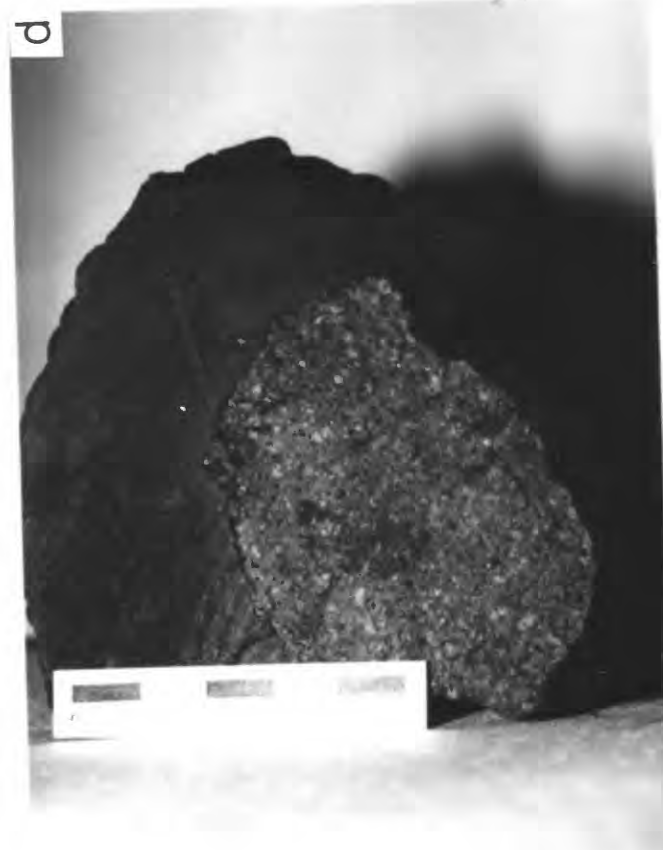
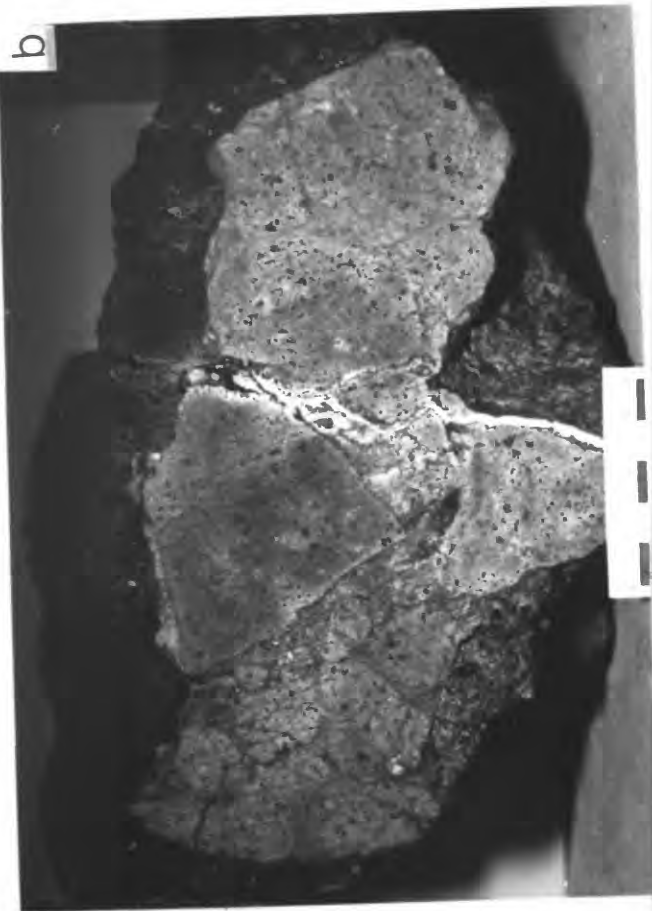


Figure 5. Manganiferous sandstone: A. D8-4, bedding plane view with botryoidal and glassy to submetallic manganese lenses. B. Cross-section of A, note submetallic, dense upper strata-bound Mn oxide layer and porous lower manganiferous sandstone layer. C. D8-15, bedding plane view with patches of submetallic Mn oxide. D. Cross-section of C with submetallic stratabound Mn oxide layers and lenses.



15

Figure 6. Manganiferous sandstone: A. D8-4, ferromanganese cement concentrated in the upper half of the bed. B. D8-12, upper brown crust 8 mm thick, middle grey, submetallic stratabound Mn oxide layer 12 mm thick, lower 10 mm thick layer of mixed manganiferous sandstone and submetallic Mn oxide oriented perpendicular to bedding that may have acted as a feeder system to the middle layer.



53

Figure 7. Submetallic to metallic manganese: A. D3-1, irregular cobble of dense, hydrothermal manganese oxide. B. D28-1, eight layers of dense hydrothermal Mn oxide encrusted with porous hydrogenetic manganese. C. D33-2-3, volcanic breccia with submetallic grey Mn oxide veins and cement. D. D52-5, stratabound Mn oxide consisting of many sublayers.

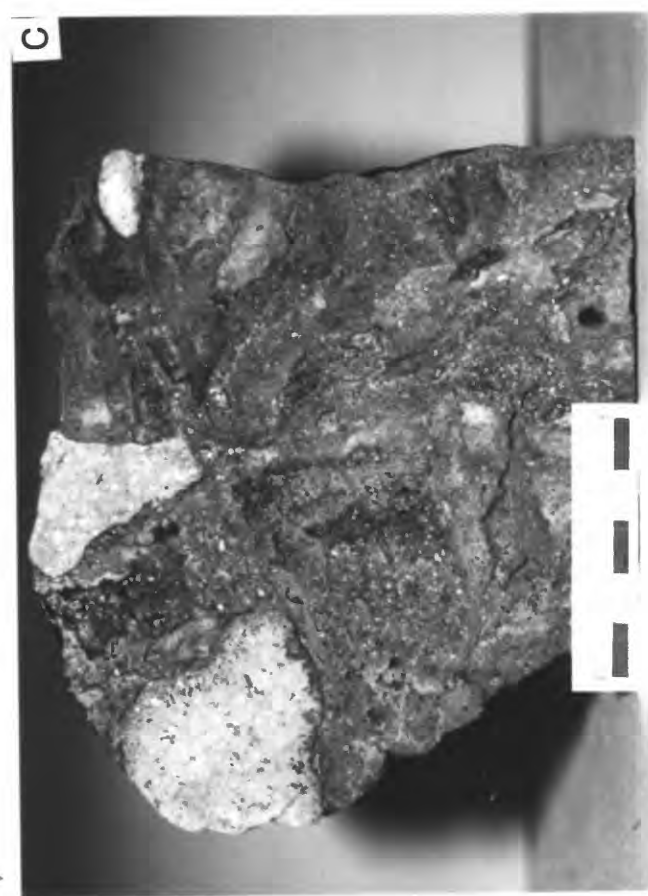


Figure 8. Chondrite-normalized rare-earth element distributions for ferromanganese crusts from the Mariana and Volcano arc. Crust thicknesses are respectively from top to bottom, 15 mm, 2 mm, 30 mm, 20 mm, 35 mm, 12 mm, 12 mm, and 20 mm.

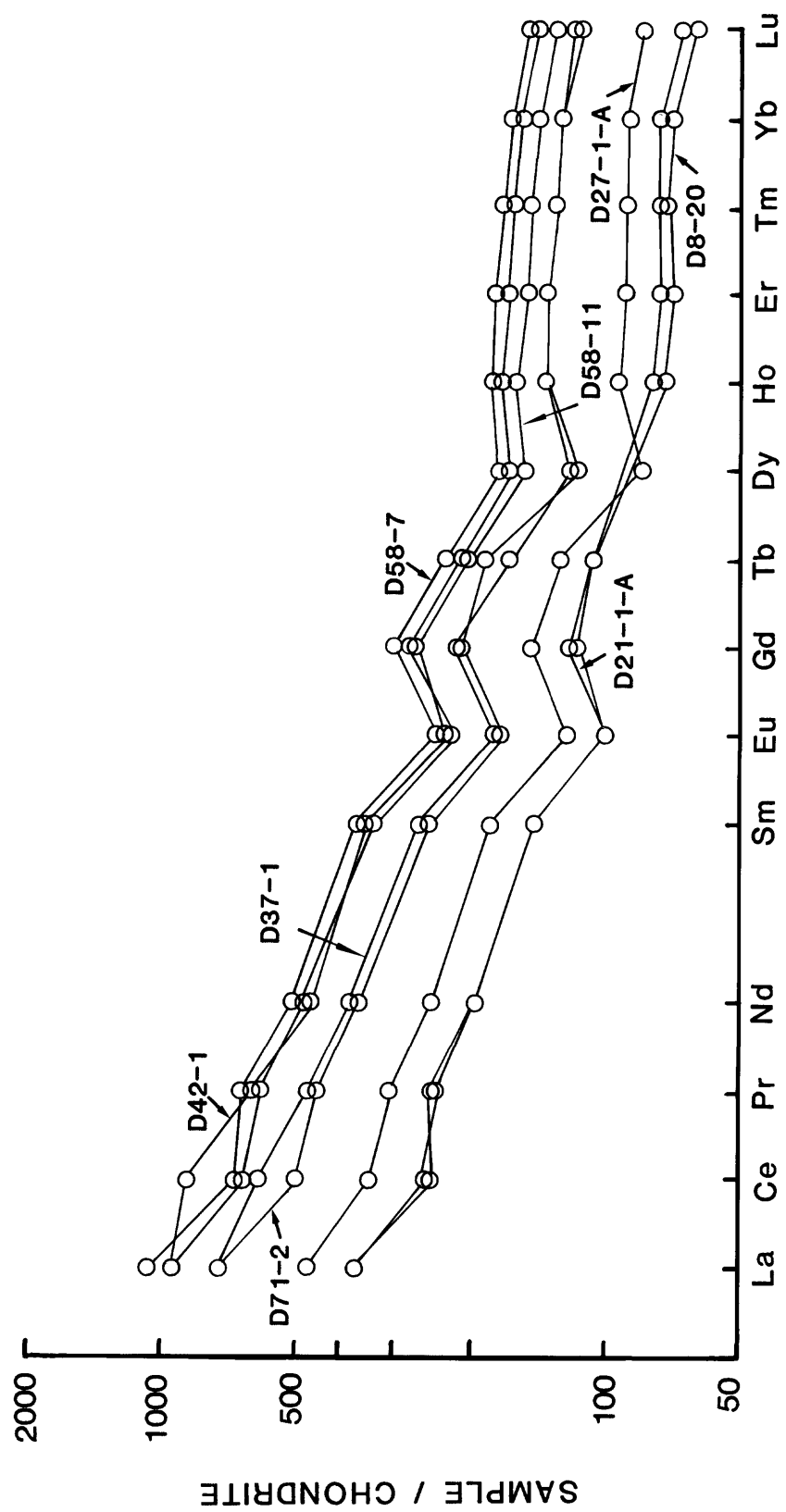


Figure 9. Chondrite-normalized rare-earth element distributions for stratabound manganese deposits from the Mariana and Volcano arcs. D28-4A, laminated, submetallic, admixed with brown ferromanganese crust and manganiferous sandstone; D41-2B-A, laminated, submetallic; D73-1F, gray to brownish-gray, laminated, submetallic; D44-1, submetallic, admixed with cement-supported manganiferous sandstone; D52-5, laminated, submetallic; D51-1, gray, laminated, submetallic, with some admixed manganiferous sandstone. Tb and Dy are below the limits of detection for D44-1.

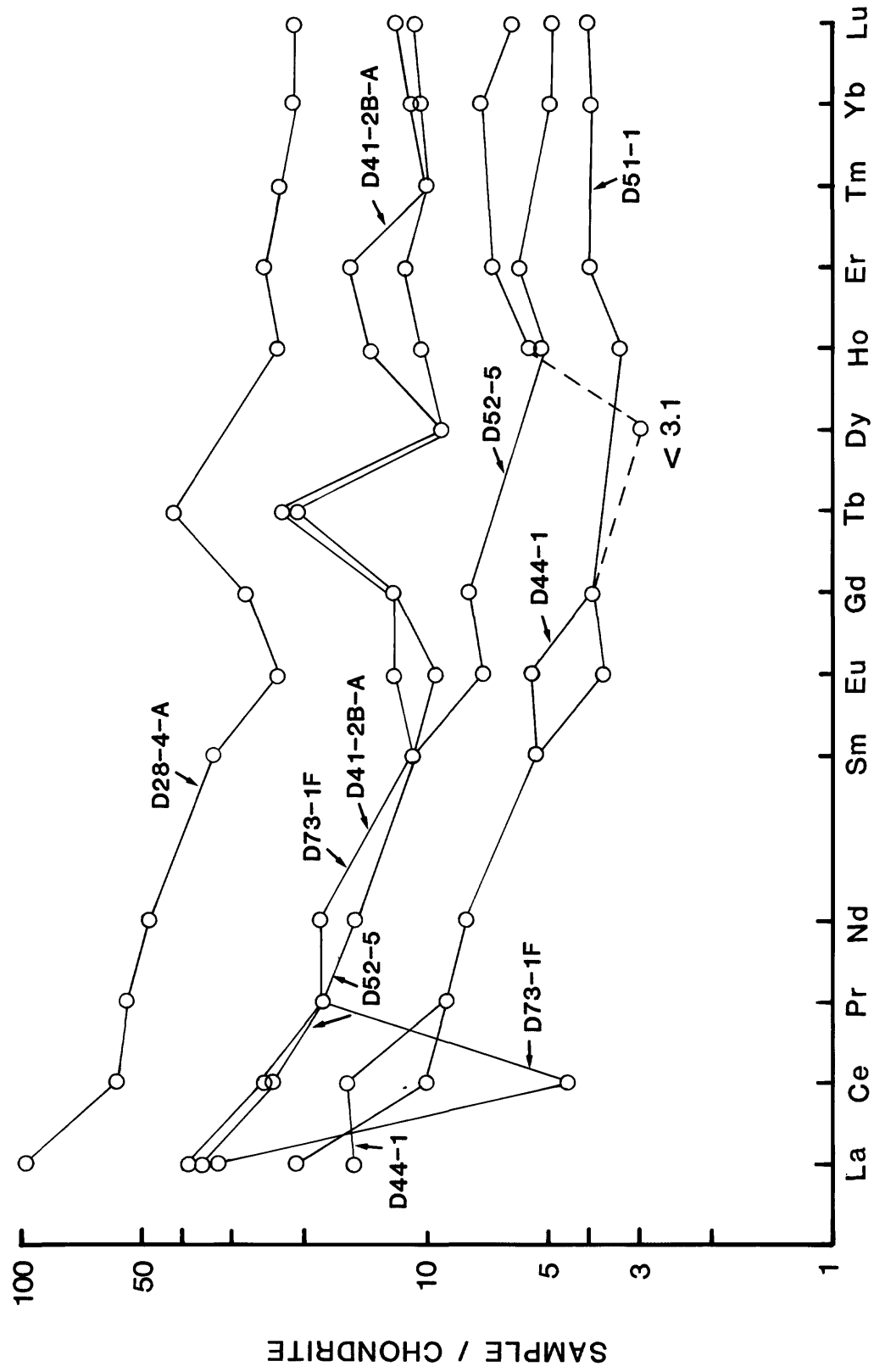


Figure 10. Chondrite-normalized rare-earth element distributions for manganiferous sandstones from the Mariana Arc. D55-3 is bedded; Tb and Dy are below the limits of detection.

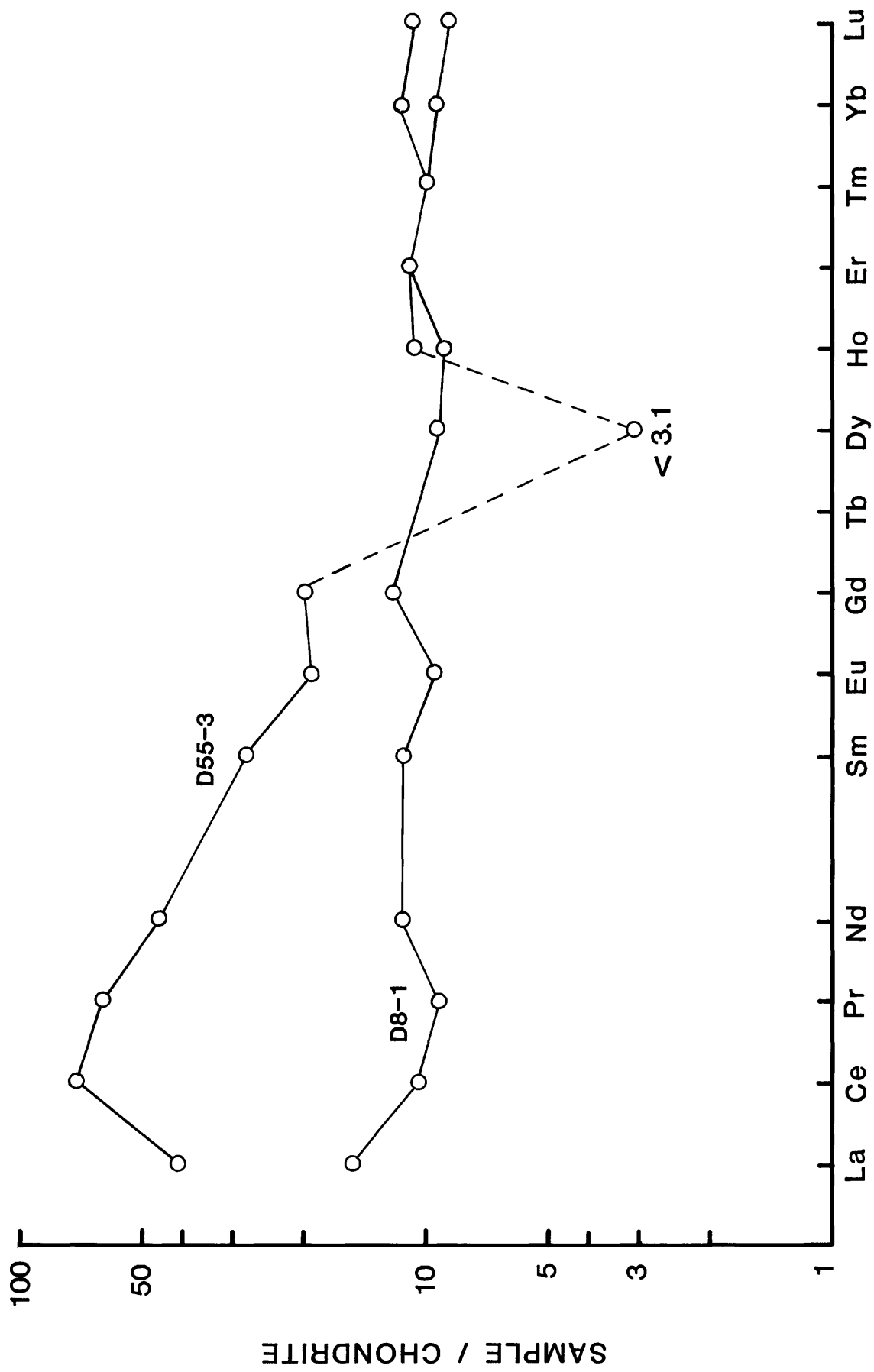
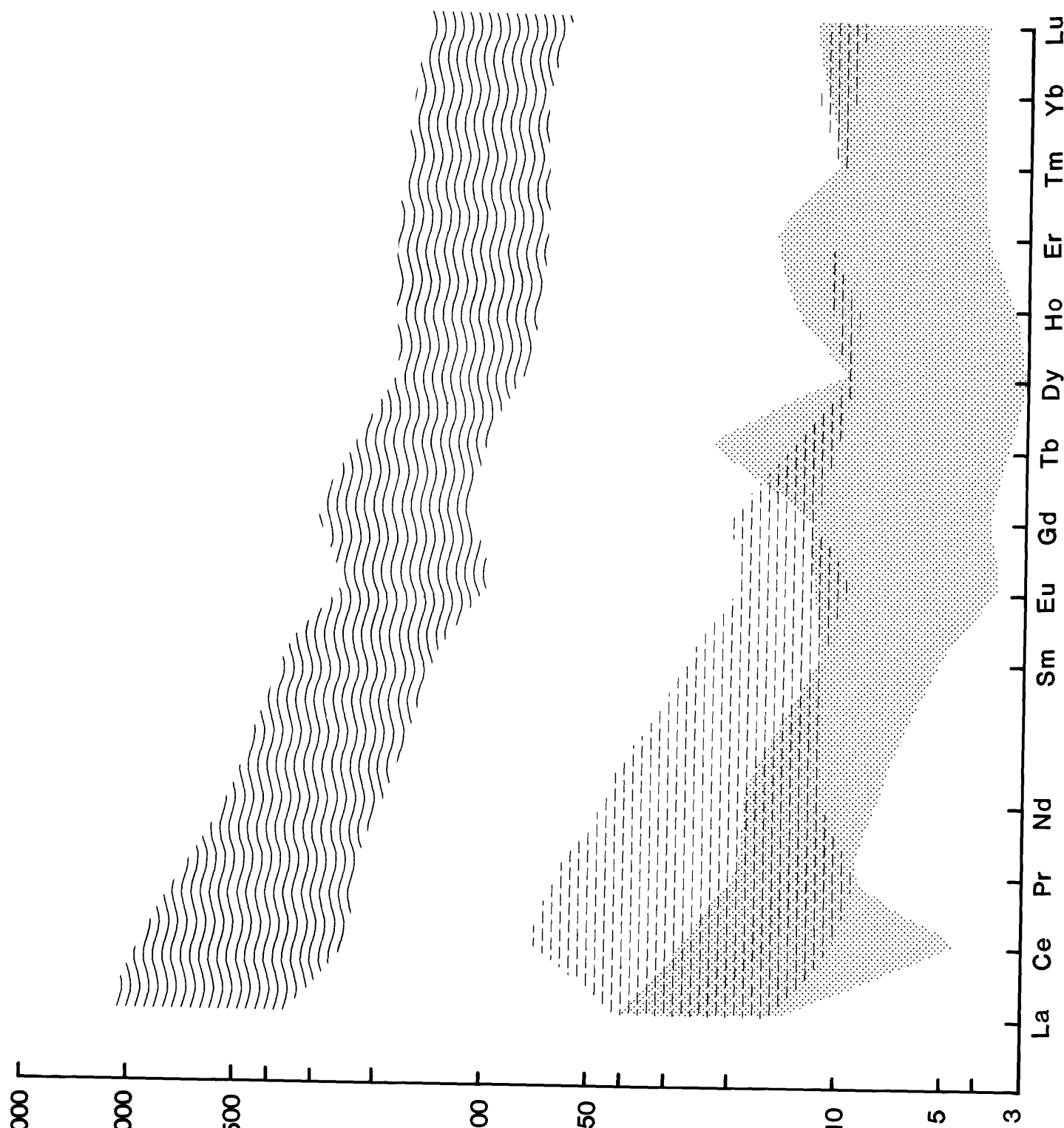
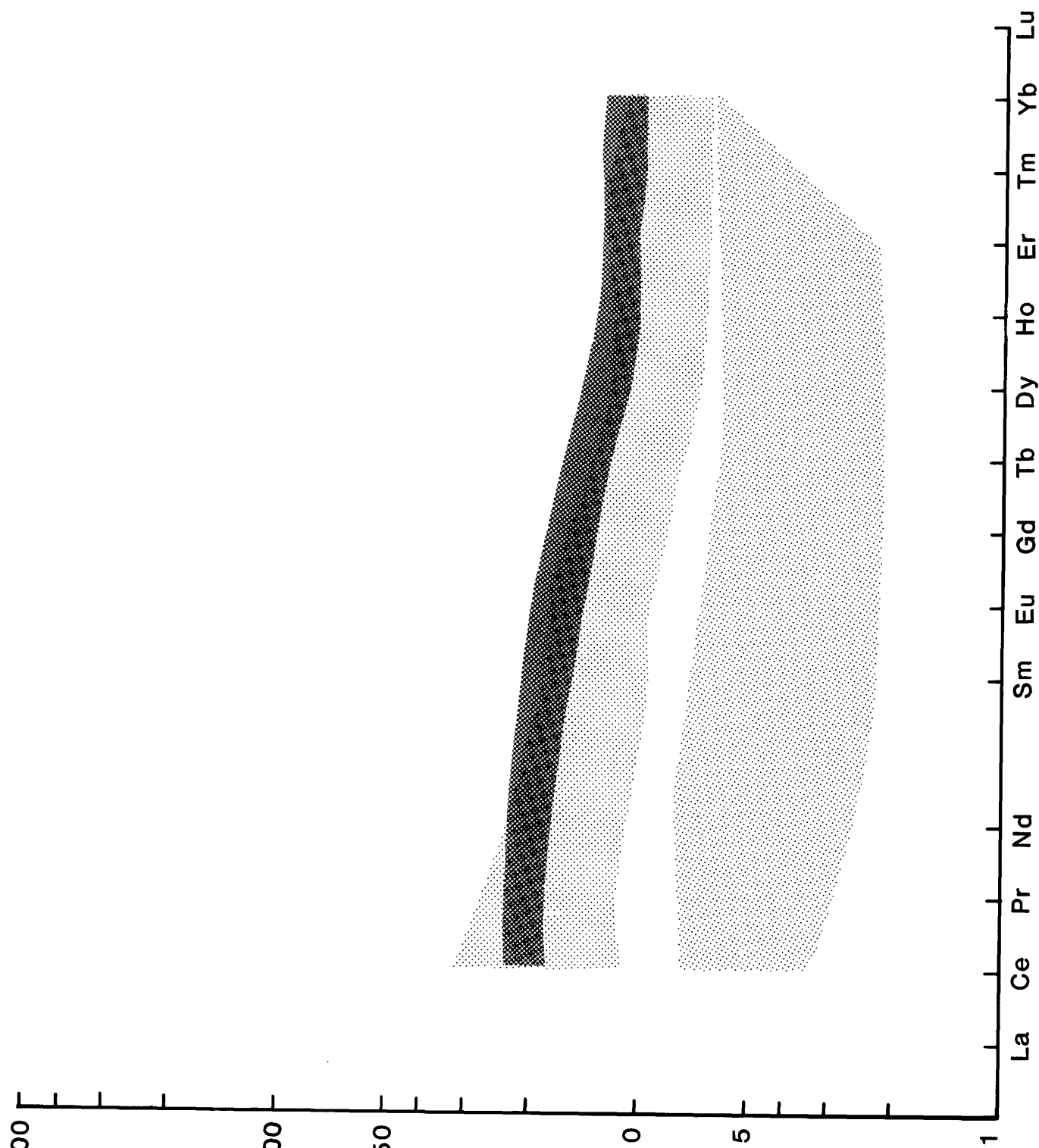


Figure 11. Chondrite-normalized rare-earth element fields for ferromanganese deposits displayed in Figures 8, 9, and 10; ferromanganese crusts (upper, wavy line), manganiferous sandstone (middle, dashed), and stratabound manganese (lower, stippled); D28-4-A is left out because it consists of a mixture of deposit types.



SAMPLE / CHONDRITE

Figure 12. Chondrite-normalized rare-earth element distribution for volcanic rocks from the Mariana Arc for comparison with the ferromanganese deposits. The lower field is for Eocene boninite and basalt (Bloomer, 1983); the upper field is for active and dormant seamounts (Dixon and Stern, 1983); the upper heavy stippled field is for rocks from the volcanically active Esmeralda Bank (Stern and Bibee, 1984).



SAMPLE / CHONDRITE

Figure 13. Ternary diagram for comparing Mn:Fe:(Cu+Ni+Co)x10 ratios for ferromanganese deposits. Hydrogenous and hydrothermal fields are from Bonatti (1972), the mid-ocean ridge crust field from Toth (1980), the Philippine Basin metalliferous sediment from Bonatti et al. (1979), the average of 10 samples from Lau Basin from Hein (1986, unpublished data), the average of 10 samples from Tonga Ridge from Hein (1986, unpublished data), and the average of 14 samples from the South China Sea from Hein (1987). The solid data represent analyses in Table 5. The most Mn-rich point represents data for 3 samples.

